Developmental Biology 394 (2014) 367–381

Contents lists available at ScienceDirect

Developmental Biology

journal homepage: www.elsevier.com/locate/developmentalbiology

Evolution of Developmental Control Mechanisms

The *Pax6* genes *eyeless* and *twin of eyeless* are required for global patterning of the ocular segment in the *Tribolium* embryo

Qing Luan [a,b], Qing Chen [a], Markus Friedrich [a,c,*]

[a] Department of Biological Sciences, Wayne State University, 5047 Gullen Mall, Detroit, MI 48202, USA
[b] Institute of Molecular Biology and Department of Chemistry and Biochemistry, University of Oregon, Eugene, OR 97403, USA
[c] Department of Anatomy and Cell Biology, Wayne State University, School of Medicine, 540 East Canfield Avenue, Detroit, MI 48201, USA

ARTICLE INFO

Article history:
Received 5 September 2013
Received in revised form
23 June 2014
Accepted 6 August 2014
Available online 19 August 2014

Keywords:
Pax6
Eyeless
Dachshund
Tribolium
Drosophila
Evolution of development
Eye
Visual system
Mushroom body
Bilaterian brain

ABSTRACT

The transcription factor gene *Pax6* is widely considered a master regulator of eye development in bilaterian animals. However, the existence of visual organs that develop without *Pax6* input and the considerable pleiotropy of *Pax6* outside the visual system dictate further studies into defining ancestral functions of this important regulator. Previous work has shown that the combinatorial knockdown of the insect *Pax6* orthologs *eyeless* (*ey*) and *twin of eyeless* (*toy*) perturbs the development of the visual system but also other areas of the larval head in the red flour beetle *Tribolium castaneum*. To elucidate the role of *Pax6* during *Tribolium* head development in more detail, we studied head cuticle morphology, brain anatomy, embryonic head morphogenesis, and developmental marker gene expression in combinatorial *ey* and *toy* knockdown animals. Our experiments reveal that *Pax6* is broadly required for patterning the anterior embryonic head. One of the earliest detectable roles is the formation of the embryonic head lobes, which originate from within the ocular segment and give rise to large parts of the supraesophageal brain including the mushroom body, a part of the posterior head capsule cuticle, and the visual system. We present further evidence that *toy* continues to be required for the development of the larval eyes after formation of the embryonic head lobes in cooperation with the eye developmental transcription factor *dachshund* (*dac*). The sum of our findings suggests that *Pax6* functions as a competence factor throughout the development of the insect ocular segment. Comparative evidence identifies this function as an ancestral aspect of bilaterian head development.

Introduction

Like most members of the Pax family of transcription factors, the *Pax6* gene is deeply conserved and characterized by two DNA binding domains: a *paired box*-domain (PAX) and a homeodomain (Kessel and Gruss, 1990; Treisman et al., 1991; Walther et al., 1991). Although executing multiple roles during development (Ashery-Padan et al., 2004; Chi and Epstein, 2002; for review see Shaham et al., 2012 and Simpson and Price, 2002), *Pax6* has drawn specific attention for its importance in the formation of visual organs (Callaerts et al., 2006; Gehring, 2012; Hanson and Van Heyningen, 1995; Hanson, 2003; Kozmik, 2008; Strickler et al., 2001). Key insights into this pivotal role have been obtained from genetic analyses in model organisms as well as of innate disorders in humans (for review see Callaerts et al., 1997; Shaham et al., 2012). In humans and mice for example, lack-of-function mutations in *Pax6* are associated with strongly defective eye development (Hill et al., 1991; Hogan et al., 1986; Lee et al., 2008; Niederfuhr et al., 1998), while in *Drosophila*, hypomorphic mutations in *Pax6* lead to complete loss of eyes (Quiring et al., 1994; Sturtevant, 1951). When misexpressed, *Pax6* can also induce ectopic eye formation not only in *Drosophila* but also *Xenopus* (Chow et al., 1999; Czerny et al., 1999; Halder et al., 1995). The fact that *Pax6* is necessary and, where tested, sufficient for initiating eye development has led to the idea that *Pax6* is a master regulator of visual organ development in bilaterian animals (Gehring, 1996).

Consistent with the master regulator view, *Pax6* is expressed in the developing visual organs of a wide range of bilaterian species (Callaerts et al., 1997). However, comparative studies have also identified photosensitive organs that develop independently of *Pax6* input based on expression analysis (Arendt et al., 2002; Backfisch et al., 2013; Blackburn et al., 2008; for review see Friedrich, 2006a; Glardon et al., 1998; Suzuki and Saigo, 2000). Functional evidence for this comes from *Drosophila,* which like insects in general, harbors two orthologs of *Pax6* (Bopp et al., 1986; Czerny et al., 1999; Quiring et al., 1994): *eyeless* (*ey*) and *twin of eyeless* (*toy*). *Drosophila ey* is expressed in the developing eye-imaginal disc, central nervous system and insulin-secreting neurons (Clements et al., 2008; Quiring et al., 1994). *Drosophila toy* overlaps with *ey* in many of these domains, but is additionally expressed in the anterior early blastoderm embryo

* Corresponding author at: Department of Biological Sciences, Wayne State University, 5047 Gullen Mall, Detroit, MI 48202, USA. Fax: +1 313 577 6891.
E-mail address: friedrichm@wayne.edu (M. Friedrich).

http://dx.doi.org/10.1016/j.ydbio.2014.08.005
0012-1606/

(Czerny et al., 1999). Further consistent with the visual organ-specific master regulator model of *Pax6* function, hypomorphic alleles of both *Drosophila ey* and *toy* are characterized by the specific depletion of the adult eye (Czerny et al., 1999; Hauck et al., 1999; Xu et al., 1999). As is characteristic of holometabolous insects, *Drosophila* also develops a separate set of larval eyes, the Bolwig's organs, that are serially homologous to the adult visual system. The Bolwig's organs, however, are not affected by *Pax6* reduction (Suzuki and Saigo, 2000). Due to the overall reduced complexity and size of the head region in the maggot-type, acephalic larva of *Drosophila*, the dispensability of *Pax6* for the development of the Bolwig's organs has been taken to suggest that *Pax6* may instead function more fundamentally as a regional patterning gene rather than a visual organ-specific regulator during insect head development (Friedrich, 2006a; Liu et al., 2006). Further consistent with this view is that much of the adult head is severely deformed in strong mutants for *Drosophila ey* or *toy* (Kronhamn et al., 2002) and that both *ey* and *toy* are expressed in a broad domain of the anterior eye disc, which encompasses but also exceeds the eye primordium proper (Bessa et al., 2002; Quiring et al., 1994).

Additional support for a regional head patterning model has been obtained from experiments in the red flour beetle *Tribolium castaneum*, another widely used model of insect development (Klingler, 2004; Richards et al., 2008). Like *Drosophila*, *Tribolium* is a holometabolous insect that develops highly reduced larval eyes in the embryo and compound eyes during postembryogenesis (Friedrich, 2006b). Unlike in *Drosophila*, however, the *Tribolium* embryo forms a complete (eucephalic) larval head capsule, representing a more ancestrally organized mode of embryonic head development (Liu et al., 2006). Consistent with the presumed ancestral function of *Pax6* in global head patterning, the reduction of *ey* and *toy* by RNA interference mediated gene knockdown (KD) not only compromises the development of both the adult eyes and the larval eyes in this system (Yang et al., 2009a), but also causes pronounced morphological abnormalities in the cuticle of the posterior larval head (Posnien et al., 2011; Yang et al., 2009a). These phenotypes are associated with the overlapping expression of *ey* and *toy* in a defined domain of the anterior embryo at blastoderm stage (Fig. 1a) (Posnien et al., 2011; Yang et al., 2009a). This expression is maintained into the embryonic head lobes: the lateral compartments of what is now widely considered the anterior-most segment of the *Tribolium* head, the ocular segment (Fig. 1b).

Recent studies have concluded that the ocular segment constitutes the anterior terminus of the procephalon (agnathal head region) in the insect head (Posnien and Bucher, 2010; Posnien et al., 2010; Snodgrass, 1935). Laterally, the anterior procephalic neuroectoderm includes the embryonic head lobes, which not only harbor the visual system primordia but also contribute to the dorsal larval head capsule (Liu and Friedrich, 2004; Posnien and Bucher, 2010; Posnien et al., 2010). The defects in the formation of the larval eyes and dorsal head bristles in combinatorial *ey* and *toy* KD *Tribolium* larvae could therefore be hypothesized to result from the perturbation of early patterning in the anterior procephalon, consistent with the model of a region-wide patterning function of *Pax6*. Until now, however, the spatial dimensions of the head patterning defects and the presumed underlying proximate defects in embryonic head patterning have not yet been precisely defined in combinatorial *ey*+*toy* KD *Tribolium* larvae. Here, we report the results of such studies, which reveal that *ey* and *toy* are redundantly required for the formation of the embryonic head lobes, which our data define as lateral derivative compartments of the ocular segment. We further provide evidence that the compromised development of the embryonic head lobes secondarily prevents the formation of its derivative tissues, which includes the larval eyes, dorsal head cuticle area, and a large part of the protocerebrum. This first genetic evidence that *Pax6* genes function as regulators of early region-wide patterning in the anterior insect head is corroborated by the loss of visual primordium-specific marker gene expression in combinatorial *ey* and *toy* KD embryos. We further demonstrate through interaction studies with the eye developmental transcription factor gene *dachshund* (*dac*) that *toy* remains required for the specific development of the larval eyes after formation of the embryonic head lobes. The sum of our findings supports a model in which *Pax6* acts as a broadly involved competence factor in the insect ocular segment, which we discuss has striking similarities in other bilaterian systems, suggesting deep ancestrality.

Materials and methods

Animals

Tribolium castaneum strains used in this work included the wild type (WT) line Georgia-1 (GA-1) and the transgenic line *pearl* pBac (3xP3-EGFP)af (Lorenzen et al., 2003; Pavlopoulos et al., 2004). Cultures were maintained as previously described (Liu and Friedrich, 2004). All analyses were carried out with 1st instar (L1) larvae.

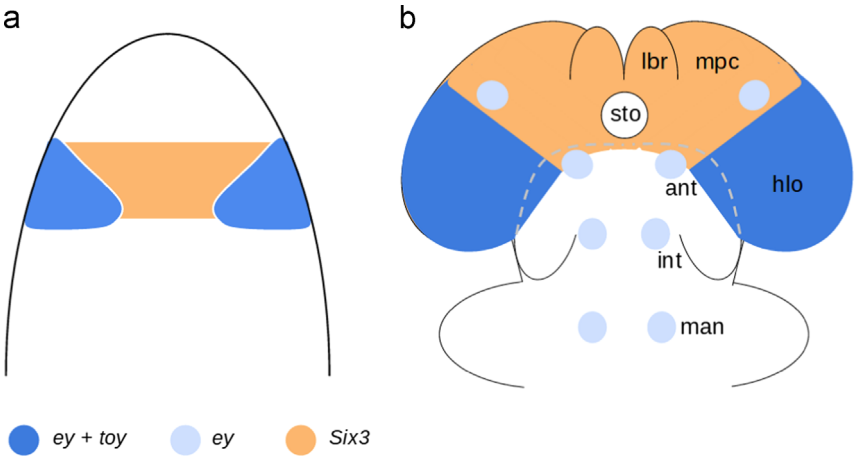

Fig. 1. Expression domains of *ey* and *toy* during embryonic head development in *Tribolium*. Schematic representation of *ey* and *toy* expression from ventral perspective in relation to the median anterior domain marker *Six3* based on Posnien et al. (2009a) and Yang et al. (2009a). Anterior is up. (a) Blastoderm stage: *ey* and toy are co-expressed in broad lateral domains of the anterior embryo. (b) Embryonic head at germband elongation stage. Hatched gray line indicates border between the anterior preoral procephalon region *sensu* Snodgrass and the posterior segmental head units. *Ey* and *toy* are coexpressed in the lateral procephalon, which are morphologically defined as the embryonic head lobes. *Ey* is, in addition, expressed in a segmental series of proneural clusters in the protocerebrum, the antennal segment, the intercalary segment, and the mandibular segment. Abbreviations: ant=antenna, hlo=head lobe, lbr=labrum, man=mandible, mpc=median protocerebrum, int=intercalary segment, sto=stomodeum.

RNA interference

Parental RNAi experiments were performed following procedures as described (Posnien et al., 2009b). For adult parental RNAi, adult females were isolated for at least three days before injection to reduce the number of older, normally developing eggs. Animals were anaesthetized with CO_2 and immobilized on tape for injection. For pupal parental RNAi, 2–3 day old female pupae were immobilized with glue (Aleene's) on slides.

Template DNA for *in vitro* transcription of dsRNA was generated by RT-PCR with primer combinations that introduced T7 RNA polymerase promoter sites through 5'-end extensions. cDNA was produced from total RNA from WT GA-1 *Tribolium* pupae extracted with the RNAqueous Kit (Ambion). The Megascript T7 reagent kit (Ambion) was used for the bidirectional *in vitro* transcription of dsRNA. dsRNAs targeting *Tribolium ey* (TC008176) corresponded the homeodomain-encoding region between nucleotides 401 and 1123 of the coding sequence (CDS) or the region between nucleotides 181–872, which encompasses both the PAX domain and homeodomain of *ey*. dsRNAs targeting *Tribolium toy* (TC007409) corresponded to the homeodomain-encoding region between nucleotides 701 and 1374 in the *toy* CDS or a ~850 bp long CDS region, which included both the PAX domain and the homeodomain. For both genes, the longer templates were amplified using generic primers targeting T7 and SP6 vector sites of clones Tc *Pax6* (RT)-pZERO and Tc-ey cDNA(A2B2) (Yang et al., 2009a). Both shorter and longer dsRNAs yielded similar KD results. The dsRNA targeting *Tribolium dac* (XP_008191786.1) was prepared as previously described (Yang et al., 2009b). CDS-specific oligonucleotides used for DNA template amplification are documented in Supplementary data file 1. Control-injections were performed with dsRNA corresponding to the CDS of the *Enhanced Green Fluorescent Protein* (*EGFP*) gene (Clontech).

Analysis of sensory head cuticle structures

The presence or absence of sensory cuticle elements in the dorsal head of L1 larvae was assessed by differential interference contrast microscopy. A reference pattern of sensory elements in the dorsal head was established by scoring 160 GA-1 L1 larva samples. The threshold condition for including elements in the reference pattern was the presence in 95% of the samples or higher. When possible, the nomenclature of Schinko et al. (2008) was adopted for the naming of specific elements. The term "alveolus" is used as defined in (Gordh and Headrick, 2011). Cuticle element 9 was not visible in 26 *Pax6* KD samples due to oblique mounting or damage and therefore not included. Pearson correlation coefficients between head reduction, larval eye depletion, and the depletion of specific head cuticle elements were calculated with the corrgram package in R (Team, 2008; Wright, 2006).

Whole mount in situ hybridization on embryos

Whole mount *in situ* hybridization was performed as previously described (Friedrich and Benzer, 2000). Template DNA for *in vitro* transcription was amplified by RT-PCR from GA-1 cDNA introducing a T7 RNA polymerase promoter site to the 5'-end of the reverse primer. Oligonucleotide sequences used for template DNA preparation are provided in Supplementary data file 1. T7 RNA polymerase (Ambion) was used for *in vitro* transcription of probes and the probes were labeled by adding digoxygenin (DIG) RNA labeling Mix (Roche) to the reaction. Anti-DIG-AP fab fragment (Roche) was used for detection and the NBT/BCIP (Promega S380C/S381C) reaction was performed for staining.

Analysis of head morphogenesis

0–36 hour old embryos were collected and fixed in 10% formaldehyde/PBS. Cellular tissue organization was visualized by labeling with Alexa Fluor 633-phalloidin (Molecular Probes, Cat#A22284). Embryos were blocked in 1 mg/ml BSA/PBT at room temperature for 1hr, followed by overnight incubation at 4 °C with Alexa Fluor 633-phalloidin diluted 1:50 in 1 mg/ml BSA/PBT.

Imaging

To inspect or image larval cuticle morphologies, larvae were collected in mineral oil and mounted live, dorsal side up. Differential interference contrast images were taken on a Zeiss Axioskope with a RT Spot camera and software (Diagnostic Instruments). Laser scanning confocal images were taken with a Leica TCS-SP2 instrument. Images were processed using Adobe Photoshop CS4.

Results

Reduction of the posterior head capsule in Pax6 knockdown Tribolium larvae

Previous studies reported abnormal dorsal bristle patterns and posterior deformations in the head capsule in *Pax6* KD *Tribolium* L1 larvae, in addition to partial or complete depletion of the larval eyes (Posnien et al., 2011; Yang et al., 2009a). This indicated additional patterning roles of *Pax6* during embryonic head development in *Tribolium* besides facilitating the formation of the visual system. To explore this, we performed parental RNAi co-injecting females with 1 μg/μl *toy* and 2 μg/μl *ey* dsRNA, which results in the reduction of all *Pax6* activity in the *Tribolium* embryo (Yang et al., 2009a). For brevity, we will refer to the combinatorial KD of *ey* and *toy* as *Pax6* KD for the remainder of the report. Consistent with the previously reported strong synergistic effect of knocking down *ey* in combination with *toy*, 78.4% of 356 investigated *Pax6* KD L1 larvae presented complete loss of both larval eyes, 16.6% loss of one larval eye, and 4.2% the reduction of photoreceptor clusters (Figs. 2b–d). In addition to the larval eye defects, 70% of the affected *Pax6* KD larvae were characterized by head capsule abnormalities. Of these, 40% presented evidence of mild (Fig. 2b,f) and 30% evidence of severe degrees of posterior head capsule reduction (Fig. 2c, d, g and h). Like the larval eye defects, the head capsule defects were frequently presented in asymmetric patterns (Fig. 2b, f and c,g). In many cases, the defects were associated with a characteristic unilateral (Fig. 2c and g) or bilateral cuticle extra-fold (Fig. 2d and h) that extended medially from the lateral head capsule. In the bilateral cases, both extra-folds merged medially, forming a neck-like groove that spanned across the posterior vertex of dorsal head (Fig. 2d and h).

No further abnormalities were detected except for the loss of the antennal flagellum in an insignificantly small number (0.3%) of *Pax6* KD larvae. Moreover, the examination of the larval head cuticles dissected from unhatched eggs ($<3\%$) did not uncover further noticeable deformities in the head region, suggesting the absence of stronger, embryonic-lethal *Pax6* KD patterning phenotypes. Taken together, these findings corroborated the previously hypothesized model of a broader role of *ey* and *toy* in the developing *Tribolium* larval head (Posnien et al., 2011; Yang et al., 2009a).

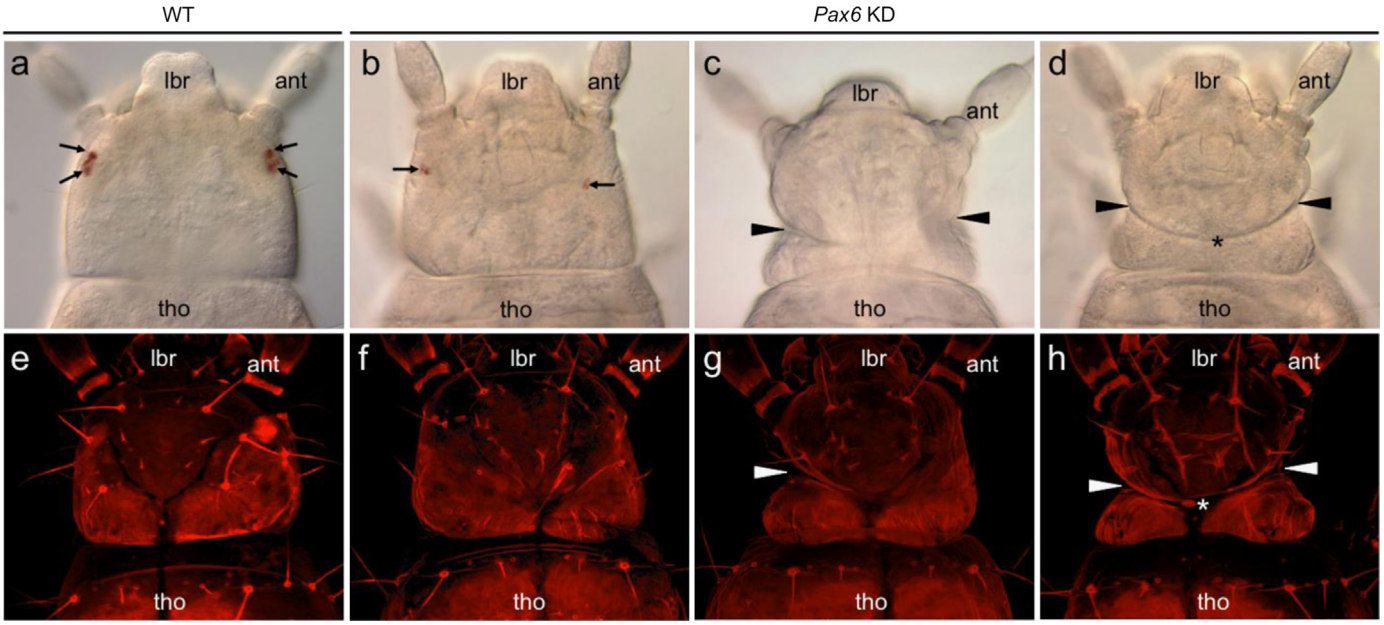

Fig. 2. *Pax6* knockdown phenotypes in the dorsal head of the *Tribolium* first instar larva. (a–h) Dorsal view. Anterior is up. (a–d) Differential interference contrast images. (a) WT specimen. The larval eyes are visible as two clusters (stemmata) of pigmented photoreceptors (arrows). (b) *Pax6* KD specimen with reduced and slightly displaced larval eyes (arrows). (c) *Pax6* KD specimen lacking larval eyes and exhibiting asymmetrical reduction of the posterior lateral head capsule leading to the formation of lateral folds (arrowheads). (d) *Pax6* KD specimen with symmetrical bilateral reduction of the lateral posterior head, associated with the formation of a 'neck'-like groove on the posterior vertex of dorsal head (asterisk). (e–h) Projections of laser scanning confocal images of cuticle autofluorescence. (e) WT specimen. (f) *Pax6* KD specimen shown in b. (g) *Pax6* KD specimen shown in c, exhibiting asymmetrical reduction of the posterior lateral head capsule (arrowheads). (h) *Pax6* KD specimen shown in d, with symmetrical bilateral reduction of the lateral posterior head. Abbreviations: ant = antenna, lbr = labrum, tho = thorax.

Pax6 knockdown deletes larval head cuticle bristles deriving from the lateral anterior embryonic procephalon

To define the *Pax6*-dependent compartments of the larval head in detail, we performed a quantitative analysis of 15 previously described sensory elements (setae, bristles, alveolae) in the dorsal head cuticle of the 1st instar larva (Fig. 3 and Supplementary data file 2) (Schinko et al., 2008). While no abnormalities of these sensory elements were detected in 59 L1 larvae from females control-injected with *EGFP* dsRNA at 3 μg/μl concentration, a selection was missing with high penetrance in *Pax6* KD offspring larvae. Like in the case of the larval eye and broader posterior head capsule abnormalities, the cuticle element depletion patterns varied between the left and right side of the head capsule of individual animals. However, no significant difference between both sides of the head was detected across all individuals examined. Therefore, numbers given below refer to the left side of the head. Rounded percentages apply to both sides of the larval head. The cuticle elements missing with the highest frequency in *Pax6* KD larvae ($>85\%$) included the posterior vertex bristle and the row bristle (elements 11 and 14, respectively), both of which are elements of the lateral head cuticle. This was followed by the loss of the more anteriorly positioned antenna basis bristle/alveolus duo and the lateral vertex seta (elements 9 and 10, respectively) in more than 65% of the larvae. The mildest deletion frequencies ranging from 30% to 40% characterized the posterior vertex setae and posterior vertex alveoli (elements 12 and 13, respectively). Finally, the most posteriorly assessed element group, the bell row, which consists of four alveoli, was present at a high frequency, although the position and specific number of the alveoli, which constitute this element, varied (element 15, compare Fig. 3b and d). Neither the signature bristles of the dorsal labrum (elements 1 and 2) nor the three cuticle elements in the vertex area (elements 3, 4, and 5), immediately posterior to the labrum, were affected in *Pax6* KD animals. The remaining elements in the vertex area (median vertex bristle, dorsomedian alveolus, and dorsomedian bristle corresponding to elements 6, 7, and 8, respectively) were challenging to score due to the extensive misfolding of the vertex cuticle in strongly affected *Pax6* KD individuals. Unlike for all other elements scored, we also noted evidence of frequent duplications as well as transformations into different morphologies for these three elements (see Supplementary data file 2). Notwithstanding these complications, depletion could be unambiguously established based on morphology and relative position and ranged below 2% for any of the three elements in the *Pax6* KD samples.

Asking whether the spatial distribution of the high-frequency deleted cuticle elements reflected localized effects or a broader, region-defining effect of *Pax6* reduction, we tested for correlations between the deletion of specific bristle elements, the depletion of the larval eyes, and the formation of extra-cuticle folds of the posterior larval head (Fig. 3e). Overall, the correlations between specific head cuticle defects were weak, reflecting a highly varied panel of individual phenotype combinations. The depletion of the larval eyes, however, was strongly correlated with the overall reduction of the posterior head as well as, more surprisingly, depletion of the posterior vertex seta (element 13). The reduction of the posterior head was likewise strongly correlated with the depletion of the posterior vertex seta but also with the depletion of the closely neighboring posterior vertex alveolus (element 12). A weaker correlation was detected between posterior head reduction and the depletion of the row bristle (element 14). Taken together, these findings suggested that the strong head reduction in *Pax6* KD larvae resulted from misregulated development of embryonic tissue that forms a region of the posterior dorsal larval head, which specifically encompasses the posterior vertex seta, the posterior vertex alveolus, the row bristle (elements 12–14) as well as the larval eyes.

Notably, the elements most affected by *Pax6* have been shown to all derive from the lateral anterior embryonic procephalon (Posnien and Bucher, 2010; Posnien et al., 2010). In further support that this area is most sensitive to *Pax6*, also the correlation between the closely neighboring posterior vertex seta and the

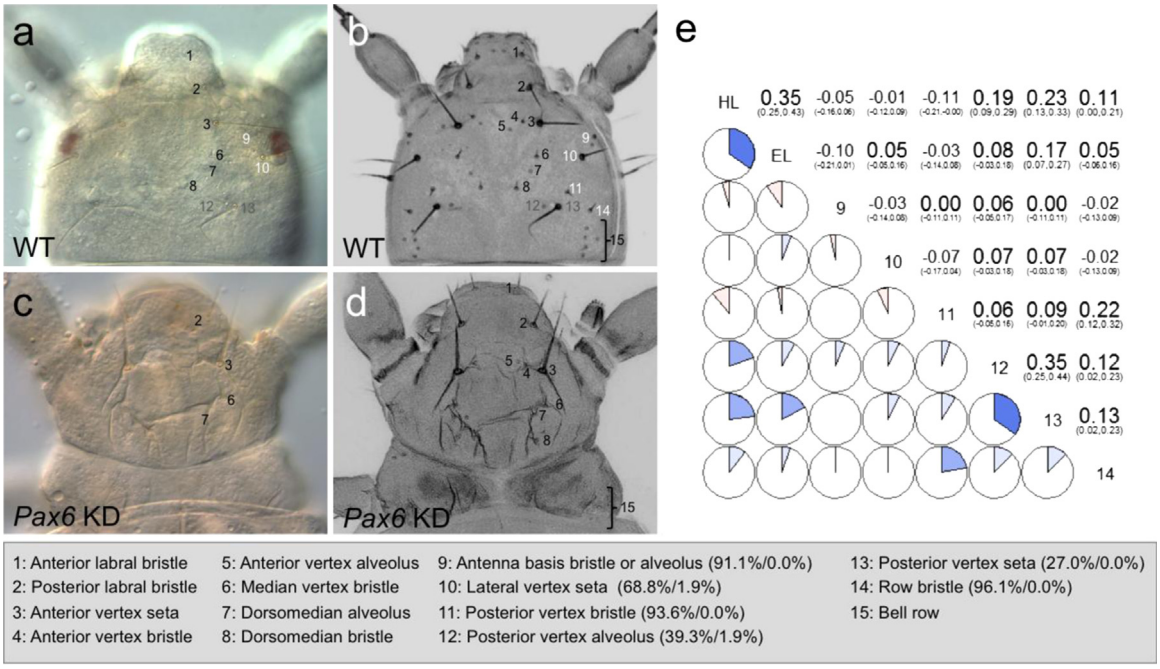

Fig. 3. Bristle pattern analysis of *Pax6* knockdown head cuticle phenotypes in *Tribolium* larvae. (a–d) Dorsal view of head cuticles of first instar larvae. Anterior up. (a and c) Differential interference contrast images. (b and d) Projections of laser scanning confocal images of cuticle autofluorescence. (a, b) WT specimen. Numbers indicate sensory cuticle elements as defined in box at the bottom. (a) Only sensory cuticle elements that are visible in focal plane chosen are labeled with numbers. (b) Same specimen as in a. Black: Elements missing in less than 5% of *Pax6* KD animals. Gray: Elements missing in more than 25% but less than 65% of *Pax6* KD animals. White: Elements missing in more than 65% of *Pax6* KD animals. Cuticle element-specific depletion penetrance on the left side of the head in experimental (first number) *versus* control animals (second number) is given in parentheses in text box for all elements missing in more than 5% of experimental animals. (c and d) An example of a *Pax6* KD specimen with strong head reduction phenotype. Numbers indicate preserved head cuticle elements. (e) Pie chart matrix summarizing correlations between reduction of the left side of the posterior head (HL), presence of the left larval eye (EL), and presence of specific sensory cuticle elements, which were missing in more than 5% of *Pax6* KD animals. Numbers in left upper quadrant show the Pearson correlation coefficient r between the two crossing elements (the numbers below represent the range of r). Pie chart color codes: Blue = positive correlation and red = negative correlation, with color hue reflecting strength of correlation.

posterior vertex alveolus (elements 12 and 13 in Fig. 3b) was high and a similarly elevated correlation was detected between the depletion of the posterior vertex bristle (element 11 in Fig. 3b) and the depletion of the row bristle (element 14 in Fig. 3b). The depletion of the latter two elements, however, was not strongly correlated with that of the closely anteriorly-positioned posterior vertex seta and posterior vertex alveolus (elements 12 and 13 in Fig. 3b), tentatively suggesting subcompartments of *Pax6*-dependent embryonic precursor tissue.

Brain defects in Pax6 knockdown larvae

The spatial organization of the *Pax6* KD-sensitive head cuticle elements suggested that their deletions reflected regulatory roles of *ey* and *toy* in the developing anterior procephalon. Since the latter also gives rise to components of the central nervous system such as the protocerebrum, we reasoned that *ey* and *toy* were also required for the development of the corresponding supraesophageal ganglia of the larval brain. To assess this, we studied the brain of transgenic *Tribolium* 3XP3-EGFP larvae, which express EGFP in a dense scaffold of glia that outlines major brain compartments (Fig. 4 and (Supplementary data file 3) (Pavlopoulos et al., 2004; Posnien et al., 2011). The supraesophageal ganglion of the L1 *Tribolium* larval head has not yet been fully described but detailed descriptions exist for the adult *Tribolium* brain (Dreyer et al., 2010) and the neuroblast fate map of the closely related darkling beetle *Tenebrio molitor* (Urbach et al., 2003). Moreover, the mushroom body anatomy has been studied in last larval and pupal *Tribolium* (Zhao et al., 2008). Drawing further on previous studies of the L1 *Tribolium* larval brain (Posnien et al., 2011), we examined eight hallmark structures which were consistently identifiable in untreated larvae ($n=4$) (Fig. 4a–d): (1) the antennal lobes, (2) the lateral protocerebral lobes, (3) the median protocerebral lobes, (4) the central body neuropil, (5) the medially juxtaposing β lobes of the mushroom body, (6) the α lobes of the mushroom body, visible in dorsal sections (Fig. 4b), (7) a ventral extension of the mushroom body, visible in ventral sections (Fig. 4d), and (8) a distinct nerve track extending in posterior direction from the antennal lobes, visible in ventral sections (4d).

Without exception, *ey* single KD, *toy* single KD as well as *Pax6* KD animals were characterized by the lack of the α lobes of the mushroom body (Fig. 4b,f,j,n). Antennal lobes, lateral protocerebrum, median protocerebrum, and central body appeared normal in *ey* and *toy* specimens (compare Fig. 4b,f,j). The β lobes of the mushroom body, however, were abnormally separated in most *ey* ($n=4$) as well as *toy* ($n=10$) KD specimens (compare Fig. 4f,j). Moreover, the ventral extensions of the mushroom bodies appeared to be missing or abnormally organized in both *ey* KD and *toy* KD animals (Fig. 4d,h,l). The same range of malformations was presented in moderately phenotypic *Pax6* KD animals defined by partial eye reduction with or without unilateral cuticle extra-fold formation in the posterior head ($n=14$) (Fig. 4m-p). However, in strongly affected *Pax6* KD animals ($n=5$), defined by the complete loss of the larval eyes and bilateral cuticle extra-folds, the supraesophageal ganglion presented a qualitatively more dramatic degree of disorganization (4q–t). Most of mushroom body elements appeared to be lacking except for highly distorted versions of the mushroom body α lobes. The central body was likewise strongly distorted and much of the lateral protocerebrum appeared reduced, precluding a clear distinction of the lateral and median protocerebral lobes (Fig. 4s and t). The antennal lobes were clearly preserved but appeared increased in size relative to the protocerebral portion of the retained supraesophageal ganglion and to untreated animals (compare Fig. 4a with r and s). Consistent with

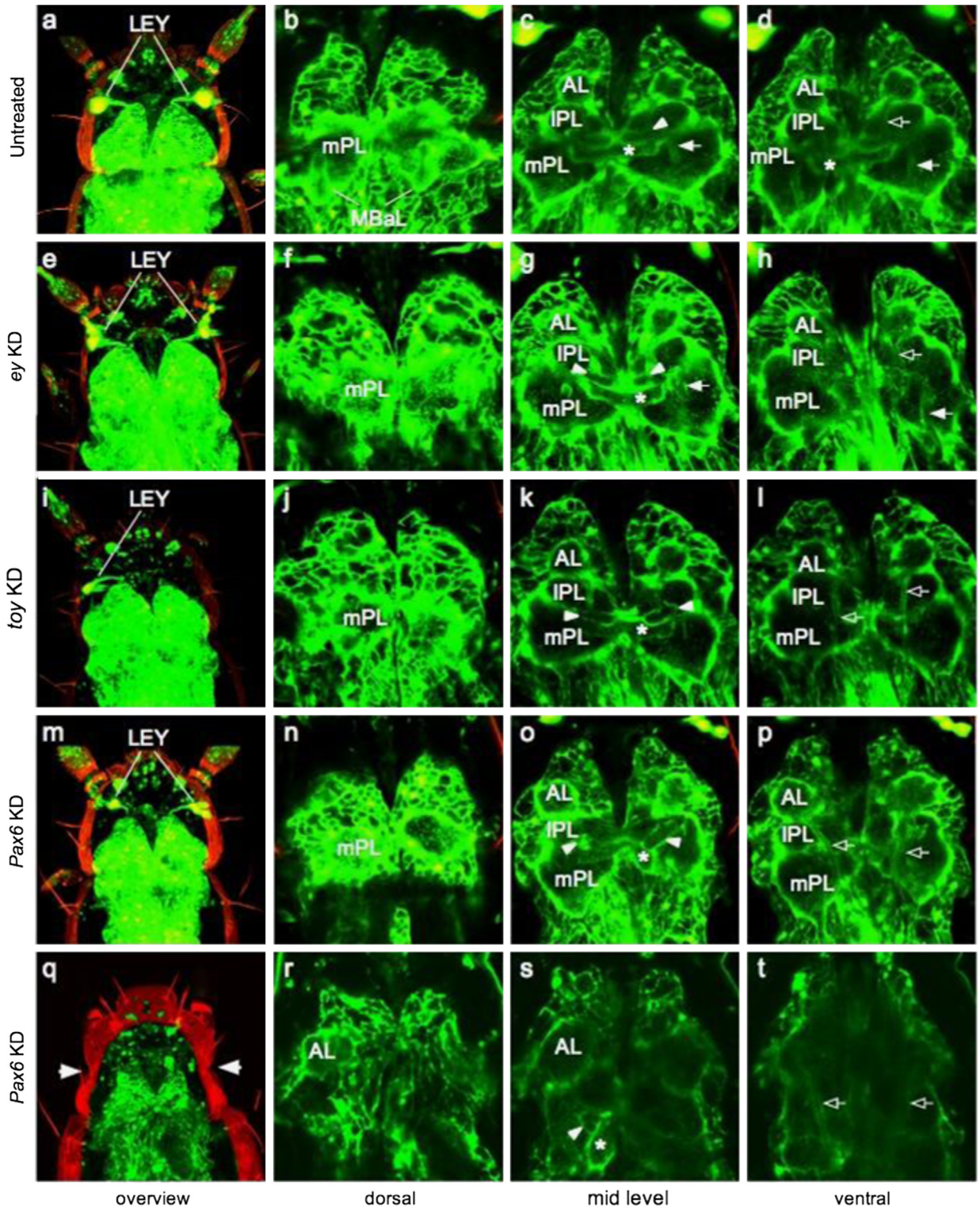

Fig. 4. Brain phenotypes in *Pax6* knockdown *Tribolium* larvae. (a–t) Confocal images of EGFP signal (green) and cuticle autofluorescence (red) from 3XP3-EGFP *Tribolium* L1 larval heads from dorsal perspective. Anterior is up. (a,e,i,m,q) Overview projection images visualizing anatomy of larval eyes, the supraesophageal ganglion, and the larval head capsule. (b,f,j, n,r) Single confocal sections in the dorsal plane of the supraesophageal ganglion. (c,g,k,o,s) Single confocal sections in the mid level plane of the supraesophageal ganglion. (d,h,l,p,t) Single confocal sections in the ventral plane of the supraesophageal ganglion. (a–d) Untreated larva with fully developed larval eyes (LEY) and all components of the supraesophageal ganglion: mushroom body α lobes (MBal) visible in dorsal level (b), antennal lobes (AL), lateral protocerebral lobe (lPL), median protocerebral lobe (mPL), the mushroom body β lobes (arrowheads in c), ventral mushroom body axon (solid arrows in c and d), and the midline spanning central body (asterisk). Axonal extensions of the antennal lobes (open arrows) are visible in d. (e–h) Strongly phenotypic *ey* KD animal. Note bilateral reduction of the larval eyes (e). Note the lack of mushroom body α lobes (f) and ventral mushroom body axons (h) as well as slight median separation of the mushroom body β lobes (g). (i–l) Strongly phenotypic *toy* KD animal characterized by unilateral larval eye loss (i). Note the lack of mushroom body α lobes (j) and ventral mushroom body axons (l) as well as median separation of the mushroom body β lobes (k) and the slight median bending of the central body (k). (m–p) Moderately phenotypic *Pax6* KD animal with bilateral eye reduction but normal posterior head capsule. Note the lack of mushroom body α lobes (n) and ventral mushroom body axons (p) as well as the severe median separation of the the mushroom body β lobes (o) and strong median bending of the central body (o). (q–t) Strongly phenotypic *Pax6* KD animal with bilateral depletion of the larval eyes and posterior cuticle extrafolds (arrowheads). The supraesophageal ganglion is strongly distorted to the effect that the median and lateral protocerebral lobes are not clearly identifiable, while the antennal lobes are enlarged (r and s). Mushroom body α lobes (r) and ventral mushroom body axons (t) undetectable. Mushroom body β lobes strongly separated and central body severely bent (s).

these severe neural defects, strongly phenotypic *Pax6* KD animals failed to exercise coordinated locomotion and died before reaching the second larval instar.

In combination, these findings revealed non-redundant roles of *ey* and *toy* in the development of specific elements of supraesophageal ganglion such as the mushroom bodies as well as a redundantly organized broader requirement for *ey* and *toy* in the development of the supraesophageal ganglion, consistent with the presumed role of both genes in the developing procephalic neuroectoderm.

Pax6 knockdown abolishes the development of the embryonic head lobes

The depletion of both peripheral and central nervous system derivatives of the anterior procephalic neuroectoderm in *Pax6* KD animals predicted patterning defects in the corresponding region during embryonic development. To probe for this, we compared the morphogenetic organization of the developing head of WT and *Pax6* KD embryos using phalloidin (Fig. 5). The earliest noticeable differences between WT and *Pax6* KD embryos were detected at the germband extension stage. In WT embryos, prominent tissue folds separate the lateral procephalic head compartments – the embryonic head lobes – from the medially adjacent antennal segment and the median protocerebrum (Fig. 5a). In *Pax6* KD embryos of the same stage (Fig. 5b), morphologically-defined embryonic head lobe compartments seemed missing and the transition between antennal and protocerebral components appeared seamless. In addition, the *Pax6* embryos were characterized by extended tissue areas in the anterior lateral head, resulting into a conspicuous triangular outline of the embryonic head. The morphology of other head compartments, such as the initiating antennal appendages, the gnathal appendages, and the condensating stomodeal opening, appeared indistinguishable between WT and *Pax6* KD embryos (compare Fig. 5a with b).

At a later stage, during early germband retraction, when the appendage-like bilateral anlagen of the labrum have formed in the anterior median head (Fig. 5c), WT embryos were characterized by further extension of the antennal and gnathal appendages, but the embryonic head lobes retained their tissue-fold separation from the antennal segment. Furthermore, in comparison to WT, *Pax6* KD embryos appeared to possess normally advanced labral, antennal, and gnathal extensions, but the embryonic head lobe compartments were partially or completely reduced (Fig. 5d). These localized lateral procephalic abnormalities persisted into subsequent stages, while the development of the labrum and the antennal segment appeared to remain unaffected (not shown). Taken together, our findings revealed that the *Pax6* KD induced defects in larval head formation manifested themselves morphologically at an early developmental time point, consistent with the predicted defects in anterior embryonic head development. Moreover, the abnormal organization of the embryonic head region pinpointed the failure of embryonic head lobe development as the proximate cause of the structural deficiencies in the posterior head of *Pax6* KD larvae.

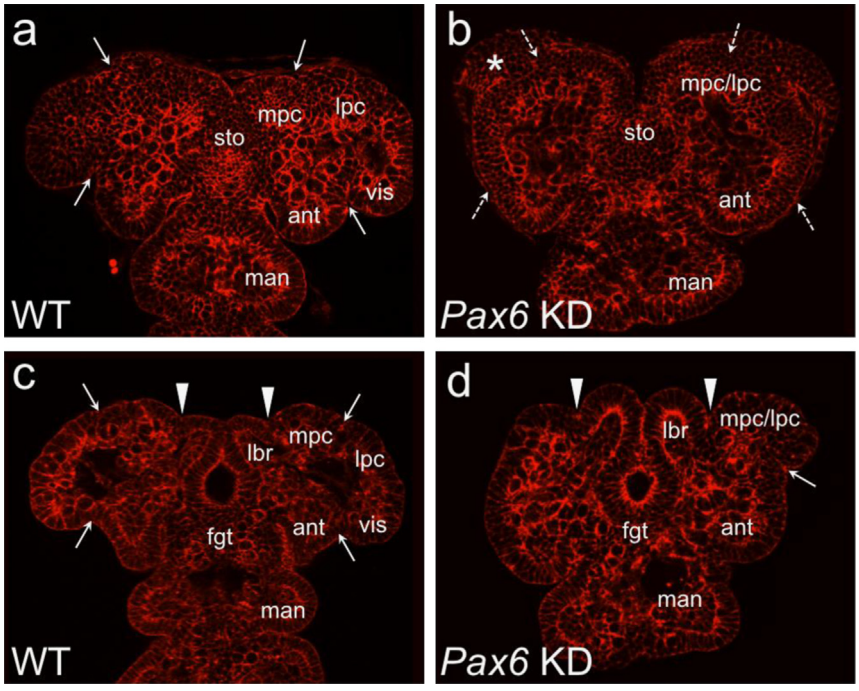

Fig. 5. Organization of the early developing head in *Pax6* knockdown embryos. (a–d) Projections of confocal image sections taken from phalloidin-labeled embryos. (a,b) Germband extension stage. The prospective stomodeal opening is defined by a cell-condensed area. (a) In control embryos, the embryonic head lobes, which contain the precursor tissues of the lateral protocerebrum and of the visual system, are defined by tissue folds (arrows) separating them from the median protocerebrum compartment at the anterior end of the embryonic head and from the antennal compartments in the posterior region of the embryonic head. (b) In *Pax6* KD embryos, the embryonic head lobe compartments are morphologically not defined (hatched arrows point at approximate position of embryonic head folds in WT embryos). Moreover, an enlarged tissue area in the lateral anterior head connects the protocerebral neuroectoderm to the extraembronic membrane (asterisk). (c,d) Progressed germband retraction stage. (c) In control embryos, the bilateral components of the future labrum have become defined, forming contact at the anterior midline. Arrowheads point at the tissue fold, which defines the lateral border between labrum and the compartment of the median protocerebrum. The stomodeal opening now marks the developing foregut. The embryonic head lobes continue to be defined by anterior and posterior tissue folds (arrows). (d) In *Pax6* KD embryos, asymmetric patterning abnormalities can be detected. In the specimen shown, tissue folds defining the embryonic head lobes are completely missing in the left hemisphere of the embryonic head. On the right side, a reduced embryonic head lobe seems to have formed, which may contain components of the median and lateral protocerebrum anlagen, as indicated by anterior and posterior tissue folds indicated by arrowheads and arrow, respectively. Abbreviations: ant=antenna, lbr=labrum, fgt=foregut, man=mandible, lpc=lateral protocerebrum, mpc=median protocerebrum, sto=stomodeum, vis=visual anlage.

Pax6 knockdown perturbs the expression of wingless in the protocerebral neuroectoderm

To obtain further insights into the perturbed embryonic head lobe development in *Pax6* KD offspring, we investigated the expression of the signaling factor gene *wingless* (*wg*), a well-defined marker of compartment organization in the embryonic insect head (Liu et al., 2006). The earliest anterior expression of *wg*, the protocerebral neuroectoderm (pne) domains, emerge on each side of the anterior head forming a bilateral pair of segmentation-like stripes, which separate the anterior most procephalon (ocular segment) from the posteriorly adjacent antennal segment (Fig. 6a). During germband extension, the pne domains disintegrate into three neuroblast precursor domains that are associated with the dorsal protocerebral neuroectoderm (dpn), the medial protocerebral neuroectoderm (mpn) and the ventral protocerebral neuroectoderm (vpn) (Fig. 6c and e). At this point, the dpn and vpn domains of *wg* demarcate the anterior and ventral borders between the developing embryonic head lobes and the median embryonic head. These landmarks correspond to future dorsal and ventral components of the larval head, respectively (Liu and Friedrich, 2004; Posnien et al., 2010). During the same time window, new compartment-specific *wg* domains emerge in the developing stomodeum, the intercalary segment, the labrum, the antennal appendages, and the gnathal segments (Fig. 6c and e).

In *Pax6* KD embryos, the early *wg* pne domains appeared not dramatically affected (Fig. 6b), consistent with the absence of morphological abnormalities in embryos preceding germband extension (Fig. 5). At mid-germband extension stage, however, the pne domains remained stripe-like in *Pax6* KD embryos instead of disintegrating into the dpn, mpn, and vpn domains (compare Fig. 6c with d). Based on the spatial correspondence to the pne domains at earlier embryonic stages in WT embryos, we interpreted these abnormal stripe-like *wg* expression domains as pne domains, which persisted in *Pax6* KD embryos (denoted pne* in Fig. 6d and f). The expression of *wg* in the labrum, antenna, intercalary, and mandible compartments was not notably different between WT and *Pax6* KD embryos, consistent with the normal morphology of their derivative structures in *Pax6* KD larvae (Figs. 2 and 3). Thus, the specific failure of the *wg* pne domains to dissociate into the dpn, mpn and vpn derivatives was hence

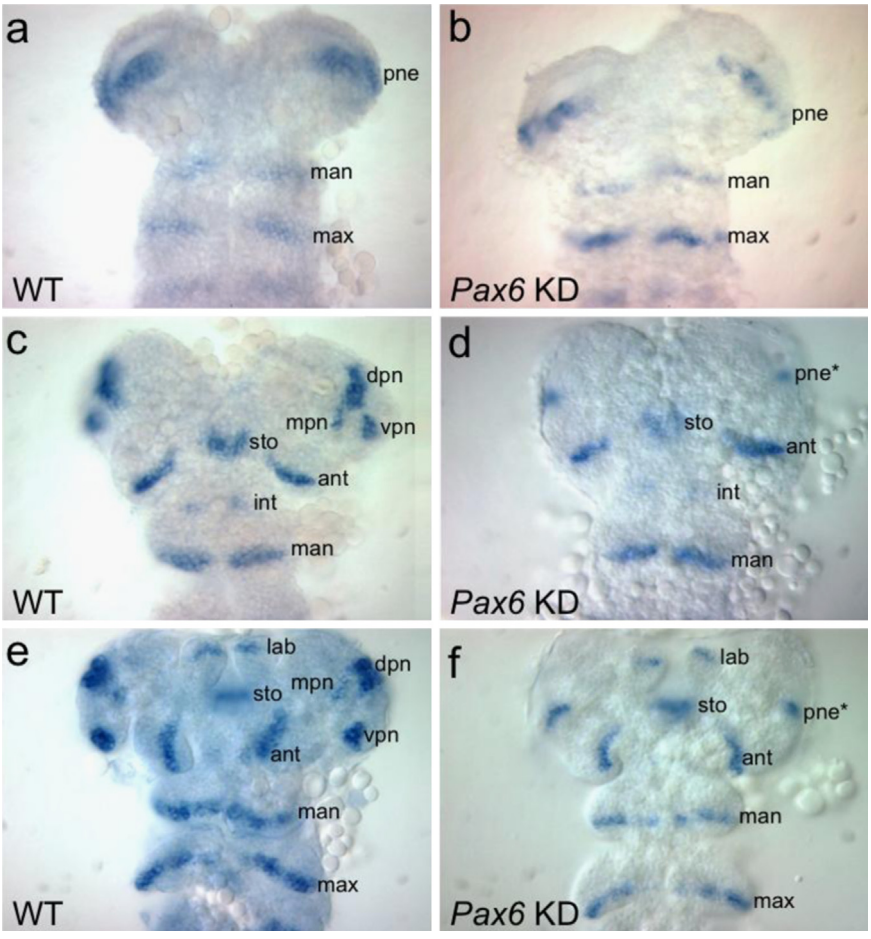

Fig. 6. *Wingless* expression in the early developing head in *Pax6* knockdown embryos. Ventral view of embryonic heads labeled by whole mount *in situ* hybridization for the expression of the *wg* gene. Anterior is to the top. Identities of *wg* expression domains indicated on the right side of each embryo with label right to each domain except for the mpn domain, where label has been placed on the left side. (a and b) Early germband extension stage. In both, the (a) WT and (b) *Pax6* KD embryo sample the procephalic pne expression domain of *wg* as well as the mandible and maxillary segment expression domains of *wg* have been formed. (c and d) Late germband extension stage. (c) In WT embryos, the pne domain has segregated into the dpn, mpn and vpn expression domains. In addition, specific *wg* expression domains are detected in the developing stomodeum, the antenna, the intercalary segment and the mandibular segment. (d) In *Pax6* KD embryos, only a single *wg* domain is detected in the lateral procephalon, suggesting the preservation of a reduced pne domain (asterisk). (e and f) Progressed germband retraction stage. (e) In WT embryos, the expression of *wg* in regions detected at the late germband extension stage (c) continues but is joined by expression in the developing labrum. (f) Also in *Pax6* KD embryos, *wg* expression corresponds to that of late germband extension stage *Pax6* KD embryos (d), including that of the reduced pne domain. Abbreviations: ant=antenna, dpn=dorsal protocerebral neuroectoderm, man=mandible, max= maxilla, mpn=median protocerebral neuroectoderm, int=intercalary segment, lab=labrum; pne=protocerebral neuroectoderm; sto=stomodeum, vpn=ventral protocerebral neuroectoderm.

consistent with the morphological evidence that the posterior head deficiencies in *Pax6* KD larvae originated from perturbed development of the embryonic head lobes.

Specific loss of marker gene expression in the embryonic head lobes of Pax6 knockdown embryos

To further scrutinize the conclusions drawn from the above morphogenesis and *wg* expression studies, we probed for the predicted lack of precursor cell populations of the visual system and the mushroom bodies by studying the expression of marker genes in *Pax6* KD embryos. The zinc finger transcription factor *disconnected* (*disco*) is specifically expressed in the early visual primordium of the *Tribolium* embryonic head at the beginning of early germband extension (Fig. 7a) (Patel et al., 2007). As the germband elongates, this expression domain of *disco* in the lateral procephalon becomes integrated into the ventral half of the embryonic head lobes (Fig. 7c and e) (Patel et al., 2007), while further expression domains initiate in the labrum and gnathal appendages (Fig. 7c and e). In *Pax6* KD embryos, the visual primordium expression domain of *disco* was missing in germband extension embryos, thus preceding the morphological definition of the embryonic head lobe compartments (Fig. 7b). The visual primordium expression domain was also missing in later embryonic stages, while the *disco* expression domains in the labrum and mandible did not differ notably to WT (compare Fig. 8a, c, and e with b, d, and f, respectively). This finding revealed the failure of visual primordium specification in *Pax6* KD embryos, in addition to and consistent with the abolishment of embryonic head lobe development.

In further support of this, we found that the embryonic head lobe-specific expression domain of the homeodomain transcription factor *intermediate neuroblast defective* (*ind*) (Wheeler et al., 2005) was absent in *Pax6* KD embryos. In *Drosophila*, *ind* expression characterizes the precursor cells of the inner optic lobe neuropil (Wheeler et al., 2005). In *Tribolium*, *ind* is expressed in a candidate patch of inner optic lobe precursor cells in the embryonic head lobe (Fig. 7g and i). This *ind*-expressing cell population could not be detected in *Pax6* KD specimens, while normal expression of *ind* was detected in neuroblast populations of the labral, antennal and gnathal head compartments (compare Fig. 7g and i with h and j, respectively).

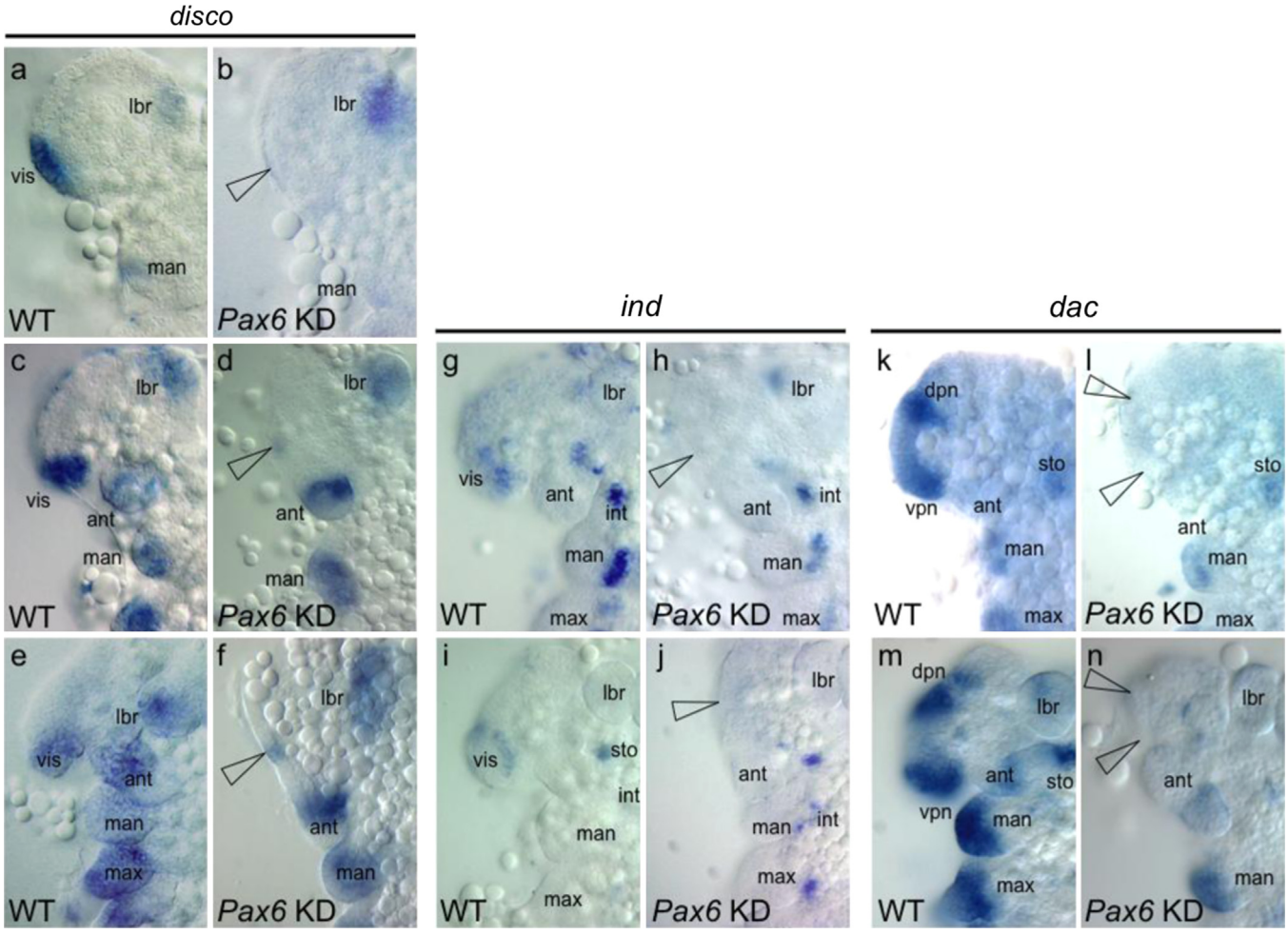

Fig. 7. Marker gene analysis of the early developing head in *Pax6* knockdown embryos. Ventral view of embryos labeled by whole mount *in situ* hybridization. Anterior is to the top. (a and b) *disco* expression in the early germband extension stage in (a) WT and (b) *Pax6* KD embryos. (c and d) *disco* expression at early germband extension in (c) WT and (d) *Pax6* KD embryos. (e and f) *disco* expression at late germband extension in (e) WT and (f) *Pax6* KD embryos. In b, d, and f, the arrowhead points towards position of the expression domain of *disco* in the visual anlage in WT embryos as seen in a, c and e, respectively. (g and h) *ind* expression at early germband extension in (g) WT and (h) *Pax6* KD embryos. (i and j) *ind* expression at late germband extension in (i) WT and (j) *Pax6* KD embryos. In h and j, the arrowhead points towards position of the expression domain of *ind* in the visual anlage in WT embryos as seen in g and i, respectively. (k and l) *dac* expression at early germband extension in (k) WT and (l) *Pax6* KD embryos. (m and n) *dac* expression at late germband extension in (m) WT and (n) *Pax6* KD embryos. In l and n, arrowheads point towards position of the expression domain of *dac* in the embryonic head lobe of WT embryos as seen in k and m, respectively. Abbreviations: ant=antenna, dpn=dorsal protocerebral neuroectoderm, man=mandible, max=maxilla, mpn=median protocerebral neuroectoderm, int=intercalary segment, lbr=labrum; pne=protocerebral neuroectoderm; sto=stomodeum, vpn=ventral protocerebral neuroectoderm.

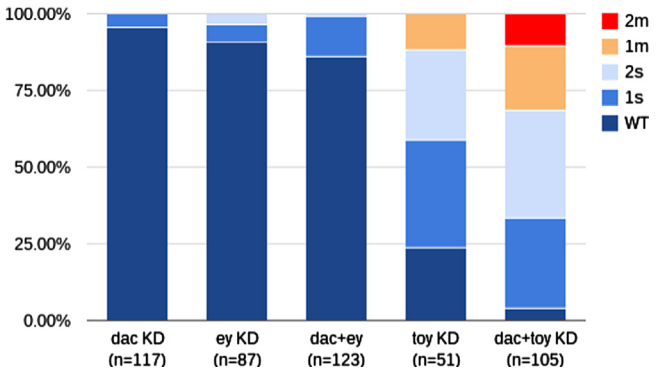

Fig. 8. Effect of combinatorial knockdown of *dac* with *ey* and *toy* on larval eye development. Bar chart describing penetrance of larval eye reduction or depletion in *ey* KD, *toy* KD, *dac* KD, *dac*+*ey* KD, and *dac*+*toy* KD animals. Abbreviations: 2m=2 missing eyes, 1m=1 eye missing, 2s=2 eyes small, 1s=one eye small.

Finally, we explored the expression of the transcription factor gene *dachshund* (*dac*) (Yang et al., 2009b), which marks both the dorsal and ventral borders of the embryonic head lobes (Fig. 7k and m). The expression domain of *dac* in the dorsal embryonic head lobe has been proposed to contribute to the mushroom body while the expression domain in the ventral head lobe maps into the visual primordium (Posnien et al., 2011; Yang et al., 2009b). Given the spatial correspondence to the dpn and vpn domains of *wg*, we refer to these expression domains as the *dac* dpn and vpn domains (compare Fig. 7c and e with Fig. 8k and m). In *Pax6* KD embryos, the *dac* dpn and vpn domains were generally highly reduced or completely absent, while the expression of *dac* in the antenna, intercalary, and mandible segments was not conspicuously altered (compare Fig. 7k and m with l and n, respectively). In summary, the embryonic head lobe-specific marker gene expression pattern analysis results verified the lack of embryonic head lobe specification as the proximate cause of the reduction of the larval head in *Pax6* KD embryos.

Combinatorial knockdown of toy and dac enhances larval eye depletion without affecting head capsule morphology

Together with the strong correlation of larval eye loss and posterior head cuticle reduction (Fig. 3e), the early effect of *Pax6* KD in the anterior procephalon suggested that the loss of larval eyes in strongly phenotypic *Pax6* KD animals was secondary to the loss of the tissue compartment in which these organs form from the visual primordia during normal development. However, larval eyes were also reduced without head capsule defects in weakly phenotypic *Pax6* KD larvae (Fig. 2b), a phenotype that has also been found in *ey* and *toy* single KD larvae (Yang et al., 2009a). These observations suggested that the development of the larval visual system continued to depend on normal *ey* and *toy* activity following successful formation of the embryonic head lobes. To scrutinize this model, we explored the effect of knocking down *ey* and *toy* in combination with *dac*, an eye developmental regulator, which lacks early patterning functions in the anterior procephalon. *dac* is expressed in the early visual primordia but can only be detected after formation of the embryonic head lobes (Fig. 7k,m) (Yang et al., 2009b).

Previous experiments targeting *dac* by parental RNAi reported the shortening of the larval legs but no major defects in the larval head (Lee et al. 2013). Consistent with this, we found no noticeable abnormalities in the posterior head capsule in our experiments. Moreover, the effect on larval eye development was very weak, with only 4.3% of *dac* KD larvae exhibiting unilateral eye reduction but no case of full eye depletion (Fig. 8). At the same time, we noted a dramatic mandible reduction phenotype at 57% penetrance (Supplementary data file 4), consistent with the strong expression of *dac* in the developing mandible (Fig. 7m) and documenting the efficacy of parental *dac* RNAi in our experiments. The combinatorial KD of *dac* with *ey* resulted in low penetrance unilateral larval eye reduction similar to that obtained in the single *ey* KD animals (Fig. 8). The combinatorial KD of *dac* with *toy*, however, produced a conspicuously stronger effect than the single KD of *toy*: 10.5% of the larvae were completely eye depleted, a phenotype that was not observed in single KD of *toy*, and the proportion of unilateral eye loss was increased to 21% in contrast to 11.8% in *toy* single KD animals. These results indicated a cooperative interaction of *dac* and *toy* in the developing larval visual system of the *Tribolium* embryo. Moreover and most importantly, none of the *dac*+*toy* KD larvae including the eye-depleted individuals showed evidence of extra fold formation in the posterior head capsule. Together, these data supported the model of a specific involvement of *toy* in the development of the larval eyes (see also Supplementary data file 3), in addition to its earlier role in embryonic head lobe development.

Discussion

Our study reveals that the *Pax6* transcription factor homologs *ey* and *toy* control early patterning events in the anterior embryonic head of *Tribolium* and that *toy* plays a later role in larval eye development. Below, we discuss implications regarding our understanding of (I–IV) the organization of the anterior insect head, (V) the role of *Pax6* in the specification of the larval eyes in *Tribolium*, (VI) the evolution of *Pax6* dispensability in higher dipterans like *Drosophila*, and (VII) the role of *Pax6* in bilaterian head and eye development.

(I) organization and development of the anterior insect procephalon

Due to the eucephalic organization of the larval head, *Tribolium* has been serving as important model for elucidating generic aspects of embryonic head development in insects (Liu et al., 2006; Posnien et al., 2010). These studies, as well as work in additional insect species (Posnien et al., 2011; Yang et al., 2009a), have converged on corroborating that the anterior agnathal insect head – the procephalon – encompasses three segments along the longitudinal body axis that are associated with segmental *wg* expression domains: (1) the antennal segment, which contains the deuterocerebrum and produces the antennal appendages, (2) the intercalary segment, which lacks appendages and contains the tritocerebrum, and (3) the ocular segment, which is marked by the *wg* pne domain (Fig. 9). Defining the ocular segment has been challenging due to its early if not immediate median split by the "anterior median region" as well as the early disintegration of its associated segmental *wg* pne domain into the non-segmental dpn, mpn and vpn domains (Fig. 6) (Liu et al., 2006). It is therefore significant that the bilateral *wg* pne domains retain segmental characteristics into later stages of development in *Pax6* KD embryos (Fig. 9b). This similarity to the continued maintenance of segmental *wg* expression in other segments further validates the ocular segment consistent with recent work in *Drosophila*, which confirmed the *wg* pne domains as parasegmental borders of the ocular segment (Ntini and Wimmer, 2011).

Our study also confirms that the ocular segment is characterized by the co-expression of *ey* and *toy* as previously suggested (Posnien et al., 2011). We further show that the ocular segment produces the embryonic head lobes and a part of the protocerebrum (Figs. 1 and 9). The integration of our results with that from previous work leads to the model of anterior *Tribolium* head development and organization outlined in Fig. 9, which

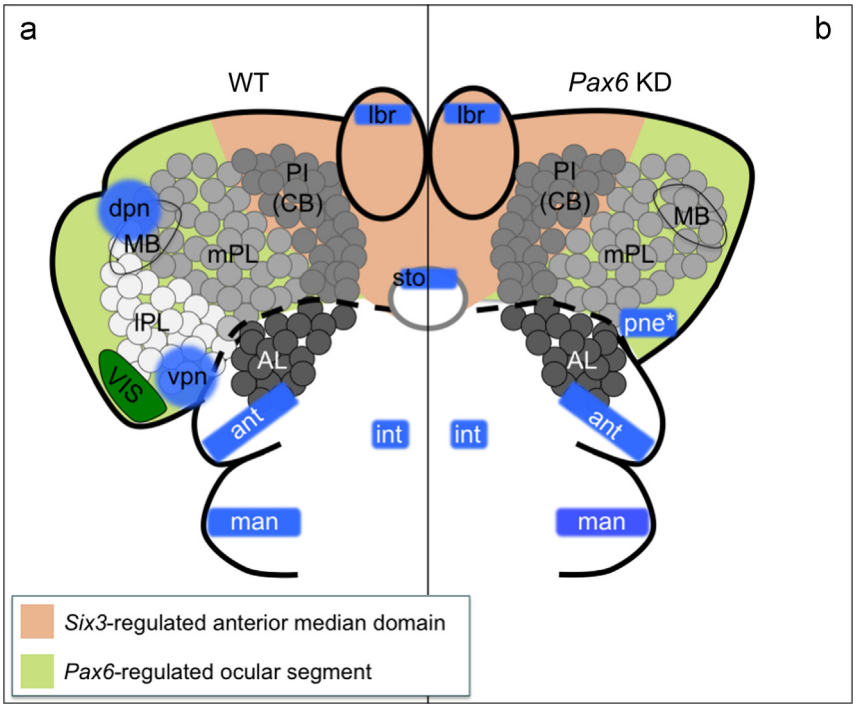

Fig. 9. A model of segment and compartment organization in the embryonic *Tribolium* head. (a) Right hemisphere of the embryonic head in a WT embryo for comparison with the (b) left hemisphere in a *Pax6 KD* animal. The neuroblast populations in the anterior embryonic head, which give rise to the different compartments of the larval supraesophageal brain, are visualized by differentially gray-colored groups of circles. Blue colored areas represent the expression domains of *wg*. White lettering on *wg* expression domains signifies the originally segmental expression domains, including the ocular segment in the protocerebral neuroectoderm (pne), the antennal segment (ant), intercalary segment (int), and the mandibular segment (man). Black lettering signifies *wg* expression domains in non-segmental structures such as the labrum (lbr) and the stomodeum (sto), and, in addition, the non-segmental derivative expression domains in the dorsal protocerebral neuroectoderm (dpn) and the ventral protocerebral neuroectoderm (vpn). In *Pax6 KD* embryos, the latter two domains (dpn and vpn) remain preserved as pne domain (pne*). Green background represents the region of the *Pax6*-regulated ocular segment. Light orange–brown background represents the *Six3*-dependent anterior median region. The comparison of the organization of the anterior head between the WT and *Pax6* KD situation highlights the specific depletion of the embryonic head lobe compartments, which incorporate the primordium of the visual system (VIS) labeled in dark green, and depicts the hypothesized depletion of the neuroblast population that gives rise to the lateral protocerebral lobe (lPL). The reduction of *Pax6* also affects the development of the mushroom bodies (MB) in which case the presumed primordium is tentatively indicated by black outline. Further abbreviations: AL=antennal lobe, mPL=median protocerebral lobe, PI=pars intercerebralis, CB=central body.

summarizes the structures and markers examined in our studies, which includes antennal lobe, median and lateral protocerebral lobe, the central body, the mushroom bodies, and the visual anlagen. Even though the central body is mildly to highly malformed in *ey*, *toy*, and *Pax6* KD animals, we conclude that the basic preservation of the central body in these KD backgrounds is consistent with the previously proposed Pax6 independence of the anterior median domain (Posnien et al., 2011). We further conclude that the central body defects seen in our KD backgrounds are the indirect effect of the strongly disturbed early patterning of the neuroectoderm in the anterior procephalon in Pax6 KD animals. This is further supported by the preservation of other structures and marker gene expression domains in the anterior median domain, most prominently the labrum.

The morphology of the mushroom bodies is affected in all of our KD treatments. This is consistent with the expression of *ey*, *toy*, and *dac* in the *wg* dpn domain area of the embryonic head lobes, which has been suggested to provide mushroom body tissue (Posnien et al., 2011). It is similarly noteworthy that we found no case of a complete reduction of the mushroom bodies. This suggests that the mushroom bodies, and possibly specific parts of it, originate from additional precursor tissue that is independent of, and thus not labeled by, the expression of *ey*, *toy*, and *dac*. Unsurprising given the complex neuroanatomy of the mushroom bodies, this aspect deserves further study.

Another suggestive finding in our experiments is the basic preservation of the median and lateral protocerebral lobes in the supraesophageal brain of *ey* or *toy* single KD animals, while strongly phenotypic *Pax6* KD animals seem to be characterized by the dramatic reduction or complete deletion of these neuropils. We suspect that these phenotypes reflect the origin of the median and lateral protocerebral lobes from the embryonic head lobes, which are only missing in the *Pax6* KD animals. However, there may be compensatory developmental flexibility regarding the recruitment of precursor neuroectoderm tissue in the anterior procephalon. We base this conjecture in part on the evidence that the antennal lobes are characterized by a relative increase in *Pax6* KD embryos and larvae consistent with a model of competitive neuroectoderm recruitment in the anterior embryonic head. While intriguing and compelling, resolving these relationships ultimately warrants challenging lineage tracing experiments.

Finally, we note the lack of evidence of compensatory expansion of signature structures of the *Six3*-defined anterior median domain: the labrum and the central body in *Pax6* KD larvae. Similarly, the relative size of the Pax6-defined median and lateral protocerebral lobes is not conspicuously different from WT in *Six3* KD larvae (Posnien et al., 2009a). These observations suggest that the ocular segment and the anterior median domain represent early independent units in the embryonic head as previously suggested (Posnien et al., 2011), consistent with the mutually exclusive expression of *Pax6* in the ocular segment and *Six3* in the median domain (Fig. 1) (Posnien et al., 2009a).

(II) morphogenetic origin of the extra cuticle folds in Pax6 KD larvae

The formation of a 'neck'-like groove is one of the most striking aspects of strongly phenotypic *Pax6* KD larvae. How does this head capsule phenotype relate to the aborted formation of the

embryonic head lobes in *Pax6* KD animals? Based on the "bend and zipper" model of insect head morphogenesis (Posnien and Bucher, 2010), the lateral and dorsal cuticle of the posterior larval head develops from the embryonic procephalon by dorsal extension, folding, and fusion, generating the Y-shaped epicranial suture (Posnien et al., 2010). The latter is considered a landmark of the boundary between the ocular segment- and labrum-derived components of the larval head. In contrast, in strongly affected *Pax6* KD larvae, the epicranial suture is replaced by the 'neck'-like groove. The lack of the development of the embryonic head lobes as the major lateral extensions of the ocular segment suggests that the ocular segment fails to contribute dorsal head cuticle in the *Pax6* KD animals, consistent with the cuticle bristle depletion phenotype of these animals. We therefore hypothesize that the 'neck'-like groove of the strongly phenotypic *Pax6* KD larvae marks the border between the dorsal head cuticle contributed by the median anterior domain, and the dorsal ridge, which is produced by the maxillary and labial segments (Posnien et al., 2009a). This model can be probed by further analyses in *Pax6* KD embryos, which would critically expand our understanding of the developmental and structural organization of the insect head.

(III) ventral appendage quality of the embryonic head lobes

The previous proposal that the embryonic head lobes represent lateral derivatives of the ocular segment (Liu et al., 2006) is supported by our finding of the correlated failure of embryonic head lobe formation and retained segmental expression of the *wg* pne domain in *Pax6* KD embryos (Fig. 9). This interpretation is further supported by a low penetrance phenotype we observed in *Pax6* KD larvae. Five of 419 sampled larvae developed a short, unilateral protrusion in the lateral head, posterior to the antennal appendage (Supplementary data file 5). While hallmark structures of specific WT appendages were not detected, the presence of circumferential areas characteristic of appendage joint sockets suggested appendage-quality. The low expressivity of this phenotype precluded us from attempting to probe for the expression of appendage patterning genes. Notwithstanding, it is tempting to speculate that these structures document an appendage-equipped ground state of the ocular segment.

Intriguingly, there is further evidence that the embryonic head lobes represent modified appendage modules. The secondary initiation of the embryonic head lobes in the ocular segment, for example, resembles the lateral initiation of ventral appendages in the gnathal and thoracic segments (Campbell et al., 1993; Ober and Jockusch, 2006). The same holds for the continued involvement of *wg* expression during early ventral appendage development. Previous studies also noted expression of appendage patterning genes such as *Distal-Less* in the early lateral procephalon (Beermann et al., 2001). The hypothesized ventral appendage character state of the embryonic head lobes could thus be further scrutinized by a targeted study of appendage patterning gene expression.

(IV) Pax6 genes as competence factors in the ocular segment of the insect head

While *ey* and *toy* have been implicated in various aspects of brain and eye development in *Drosophila* (Callaerts et al., 2001; Furukubo-Tokunaga et al., 2009), our data provide the first evidence of a role of these genes in the early compartmentalization of a segment in the insect head. This finding opens the question of how *ey* and *toy* impact the patterning of the ocular segment at the gene regulatory and morphogenetic level. Several lines of evidence lead to the conclusion that the sum of the defects in the head of *Pax6* KD larvae is caused by a single primary defect: The formation of the embryonic head lobes as distinct compartments of the ocular segment. At the gene expression level, this model is supported by the overlapping expression of *ey* and *toy* in the early ocular segment, which continues into the embryonic head lobes (Yang et al., 2009a). At the level of gene function, this model is supported by the specific reduction or loss of the embryonic head lobes in combinatorial *Pax6* KD embryos. This large-scale embryonic phenotype is associated with the reduction or loss of gene expression domains that mark subcomponents of the embryonic head lobes, including the visual system (*disco*) and the mushroom bodies (*dac*), thus explaining the reduction or loss of these structures in the mature larval head of experimental animals. Finally, the previously demonstrated link between the embryonic neuroectoderm of the lateral procephalon and the dorsal cuticle of the larval head (Posnien and Bucher, 2010) connects the head bristle abnormalities in combinatorial *Pax6* KD larvae to the mispatterning of the lateral procephalon.

We predict that understanding the regulation and function of the dynamic development of the *wg* pne expression domain will be key to understanding the compartmentalization of the ocular segment and the role of *Pax6* in this process. Given the dramatic reduction of the ocular segment-related *wg* expression domains in *Drosophila* (Liu et al., 2006; Ntini and Wimmer, 2011), studying these processes will be reserved to models with eucephalic embryonic head development like *Tribolium* (Liu et al., 2006; Posnien et al., 2010). Indeed, additional tentative conclusions can already be drawn from the data produced in this study. The preservation of the segmental pne domain in *Pax6* KD animals, for example, implies that *ey* and *toy* are not required for the establishment of the ocular segment as such. However, the lack of the visual system expression domain of *disco*, which originates prior to the formation of the embryonic head lobes during normal development, reveals that the activity of *ey* and *toy* is required for region-specific gene activation in the ocular segment already before the morphological definition of the embryonic head lobes. The same is true for the *Pax6*-dependent separation of the *wg* pne domain. These observations lead to a model in which the *Pax6* genes *ey* and *toy* function as permissive or competence factors that allow for proper compartmentalization in the ocular segment, which likely involves the local activation and integration of signaling pathway activities.

(V) indirect and specific requirements of Pax6 for larval eye development in Tribolium

A key motivation of our study was to elucidate whether *ey* and *toy* are directly or indirectly required for the development of the larval eyes in *Tribolium*. We previously hypothesized that the sensitivity of larval eye development to *Pax6* reduction in *Tribolium* was the indirect consequence of the broad effect of *Pax6* reduction on the development of the anterior head as opposed to a specific role in the differentiation or specification of the larval eyes (Yang et al., 2009a). The results obtained here confirm that the depletion of the larval eyes in strong *Pax6* KD is the indirect consequence of the compromised development of the embryonic head lobes. Notwithstanding, a continued, later requirement of *ey* and *toy* for the specification of the visual system and eventually the larval eye primordia is supported by the following observations and findings: (1) the persisting expression of *ey* and *toy* in the developing embryonic head lobes; (2) the specific reduction or depletion of the larval eyes in *ey*, *toy*, and *Pax6* KD animals with normal head capsule morphology, which implies continued *Pax6* dependence of the larval visual system in embryos in which the embryonic head lobes undergo otherwise normal development; (3) the synergistic effect of the combinatorial KD of *toy* with *dac* on larval eye loss which likewise has no strong effect on head capsule

morphology. Our study thus both confirms the indirect requirement of *ey* and *toy* for the development of the larval eyes in *Tribolium* as well as their continued requirement to serve as competence factors in the precursor cell populations of the larval eyes.

Of note, our analysis of brain phenotypes indicate similar indirect and direct *Pax6* requirements for the development of the mushroom bodies (Supplementary data file 3). This is expected assuming evolutionary conservation of the mushroom body patterning functions characterized in *Drosophila* as well as considering the expression of *dac* in mushroom body precursor regions of the embryonic head lobes in *Tribolium* (Fig. 7k and m) (Yang et al., 2009b). The approach taken here should be straightforward to apply to the deeper comparative study of mushroom body and anterior brain development in *Tribolium*.

(VI) an expanded model explaining the loss of larval eye Pax6 dependence in the acephalic Higher Diptera

It has been previously proposed that the dispensability of *ey* and *toy* for the development of the larval eyes in *Drosophila* resulted from the extreme reduction of the embryonic head and its patterning during dipteran evolution (Friedrich, 2006a; Yang et al., 2009a). This model was based on the presumed indirect dependence of larval eye development on *ey* and *toy* in species with ancestral eucephalic larval head morphology such as *Tribolium*. Interestingly, this model is in part further validated by the stalled *wg* pne domain in *Pax6* KD embryos. Comparative evidence implies that this domain is homologous to the so-called "head blob" domain in the developing procephalon of the *Drosophila* embryo, which, similar to the *Pax6* KD embryos, is associated with the reduction of the embryonic head lobes in higher Diptera (Liu et al., 2006). The reduction of the embryonic head lobes in *Pax6* KD embryos can thus be viewed as an experimental replica of evolutionary developmental change that molded the acephalic dipteran head. This is further supported by the associated loss of the blastoderm phase of *ey* expression in the *Drosophila* ocular segment (Quiring et al., 1994; Yang et al., 2009a).

However, our additional finding of the continued requirement of *toy* for the development of the larval eyes in *Tribolium* implies that a reduction of the embryonic procephalon does not entirely liberate larval eye development from the dependence of an early competence input by *ey* and *toy*. We therefore propose that the evolution of *Pax6*-independence of larval eye development in the acephalic dipteran larvae involved further gene regulatory reorganization that freed the development of the larval eyes from the ancestral direct dependence on *Pax6* activity during specification. This expanded model of the developmental evolution of the larval eye in the higher Diptera could be further tested by comparing the cis-regulatory requirements of early photoreceptor differentiation genes during larval and adult eye development in *Drosophila*, which our model predicts to differ in substantial ways. A particularly interesting candidate coming to mind is the proneural transcription factor *atonal*, which is directly activated by *ey* during adult eye development (Zhang et al., 2006; Zhou et al., 2014).

(VII) Pax6 a master regulator of anterior brain development

While the evidence of the roles of *ey* and *toy* in the early compartmentalization of the anterior embryonic head in insects presented here is new, it is reasonable to assume that many of the related and later roles of *ey* and *toy* in the ocular segment of *Tribolium* are homologous to functions of *ey* and *toy* in the development of the brain and adult head in *Drosophila* (Callaerts et al., 2001; Furukubo-Tokunaga et al., 2009; Kronhamn et al., 2002). It is also important to note that *Pax6* regulates early compartmentalization and other patterning processes in the developing forebrain of vertebrates (for review see Manuel and Price, 2005; Osumi et al., 1997; for review see Osumi et al., 2008; Pratt and Price, 2006; Simpson and Price, 2002; Stoykova et al., 1996; Walther and Gruss, 1991). These anchor points from model organisms are complemented by consistent expression pattern evidence that *Pax6* regulates patterning of the anterior embryonic head throughout the Bilateria (Arendt et al., 2002; Eriksson et al., 2013; Lowe et al., 2003; Passamaneck et al., 2011; Quigley et al., 2007; Schlosser, 2005). The comparative evidence is thus unequivocal that the anterior brain patterning function by *Pax6* dates back to the developmental program of the bilaterian ancestor. We therefore conclude that the patterning of the ocular segment by *ey* and *toy* in *Tribolium* reflects an ancestral function of *Pax6* in bilaterian brain development. Given the regressive evolution of this function in *Drosophila*, our study thus further corroborates the value of *Tribolium* for elucidating ancestral mechanisms of animal head development.

Acknowledgments:

We thank Harshal Vora and Jeremiha Fowler for help with bristle phenotype analysis, Bill Branford, Tiffany Cook, and the anonymous reviewers for helpful comments on the manuscript. QL was supported by a Thomas C. Rumble Fellowship from Wayne State University. The project was supported by NSF Grant IOS 0951886.

Appendix A. Supporting information

Supplementary data associated with this article can be found in the online version at http://dx.doi.org/10.1016/j.ydbio.2014.08.005.

References

Arendt, D., Tessmar, K., de Campos-Baptista, M.I., Dorresteijn, A., Wittbrodt, J., 2002. Development of pigment-cup eyes in the polychaete *Platynereis dumerilii* and evolutionary conservation of larval eyes in Bilateria. Development 129, 1143–1154.

Ashery-Padan, R., Zhou, X., Marquardt, T., Herrera, P., Toube, L., Berry, A., Gruss, P., 2004. Conditional inactivation of *Pax6* in the pancreas causes early onset of diabetes. Dev. Biol. 269, 479–488.

Backfisch, B., Rajan, V.B.V., Fischer, R.M., Lohs, C., Arboleda, E., Tessmar-Raible, K., Raible, F., 2013. Stable transgenesis in the marine annelid *Platynereis dumerilii* sheds new light on photoreceptor evolution. Proc. Natl. Acad. Sci. 110, 193–198.

Beermann, A., Jay, D.G., Beeman, R.W., Hulskamp, M., Tautz, D., Jurgens, G., 2001. The *Short antennae* gene of *Tribolium* is required for limb development and encodes the orthologue of the *Drosophila* Distal-less protein. Development 128, 287–297.

Bessa, J., Gebelein, B., Pichaud, F., Casares, F., Mann, R.S., 2002. Combinatorial control of *Drosophila* eye development by *eyeless*, *homothorax*, and *teashirt*. Genes Dev. 16, 2415–2427.

Blackburn, D.C., Conley, K.W., Plachetzki, D.C., Kempler, K., Battelle, B.Ä., Brown, N.L., 2008. Isolation and expression of *Pax6* and *atonal* homologues in the American horseshoe crab, *Limulus polyphemus*. Dev. Dyn. 237, 2209–2219.

Bopp, D., Burri, M., Baumgartner, S., Frigerio, G., Noll, M., 1986. Conservation of a large protein domain in the segmentation gene paired and in functionally related genes of *Drosophila*. Cell 47, 1033–1040.

Callaerts, P., Clements, J., Francis, C., Hens, K., 2006. *Pax6* and eye development in Arthropoda. Arthropod Struct. Dev. 35, 379–391.

Callaerts, P., Halder, G., Gehring, W.J., 1997. PAX-6 in development and evolution. Annu. Rev. Neurosci. 20, 483–532.

Callaerts, P., Leng, S., Clements, J., Benassayag, C., Cribbs, D., Kang, Y., Walldorf, U., Fischbach, K.F., Strauss, R., 2001. *Drosophila* Pax-6/eyeless is essential for normal adult brain structure and function. J. Neurobiol. 46, 73–88.

Campbell, G., Weaver, T., Tomlinson, A., 1993. Axis specification in the developing *Drosophila* appendage: The role of *wingless*, *decapentaplegic*, and the homeobox gene *aristaless*. Cell 74, 1113–1123.

Chi, N., Epstein, J.A., 2002. Getting your Pax straight: Pax proteins in development and disease. Trends Genet. 18, 41–47.

Chow, R.L., Altmann, C.R., Lang, R.A., Hemmati-Brivanlou, A., 1999. *Pax6* induces ectopic eyes in a vertebrate. Development 126, 4213–4222.

Clements, J., Hens, K., Francis, C., Schellens, A., Callaerts, P., 2008. Conserved role for the *Drosophila Pax6* homolog Eyeless in differentiation and function of insulin-producing neurons. Proc. Natl. Acad. Sci. USA 105, 16183–16188.
Czerny, T., Halder, G., Kloter, U., Souabni, A., Gehring, W.J., Busslinger, M., 1999. *twin of eyeless*, a second Pax-6 gene of *Drosophila*, acts upstream of *eyeless* in the control of eye development. Mol. Cell 3, 297–307.
Dreyer, D., Vitt, H., Dippel, S., Goetz, B., El Jundi, B., Kollmann, M., Huetteroth, W., Schachtner, J., 2010. 3D standard brain of the red flour beetle *Tribolium castaneum*: a tool to study metamorphic development and adult plasticity. Front. Syst. Neurosci. 4.
Eriksson, B.J., Samadi, L., Schmid, A., 2013. The expression pattern of the genes *engrailed*, *pax6*, *otd* and *six3* with special respect to head and eye development in *Euperipatoides kanangrensis* Reid 1996 (Onychophora: Peripatopsidae). Dev. Genes Evol., 1–10.
Friedrich, M., 2006a. Ancient mechanisms of visual sense organ development based on comparison of the gene networks controlling larval eye, ocellus, and compound eye specification in *Drosophila*. Arthropod Struct. Dev. 35, 357–378.
Friedrich, M., 2006b. Continuity *versus* split and reconstitution: exploring the molecular developmental corollaries of insect eye primordium evolution. Dev. Biol. 299, 310–329.
Friedrich, M., Benzer, S., 2000. Divergent *decapentaplegic* expression patterns in compound eye development and the evolution of insect metamorphosis. J. Exp. Zool. 288, 39–55.
Furukubo-Tokunaga, K., Adachi, Y., Kurusu, M., Walldorf, U., 2009. Brain patterning defects caused by mutations of the *twin of eyeless* gene in *Drosophila melanogaster*. Fly (Austin) 3, 263–269.
Gehring, W.J., 1996. The role of *eyeless* as a master control gene in eye morphogenesis and evolution. Dev. Biol. 175 (P1-P1).
Gehring, W.J., 2012. The evolution of vision. Wiley interdisciplinary reviews. Dev. Biol. , http://dx.doi.org/10.1002/wdev.1096.
Glardon, S., Holland, L.Z., Gehring, W.J., Holland, N.D., 1998. Isolation and developmental expression of the *Amphioxus* Pax-6 gene (AmphiPax-6): insights into eye and photoreceptor evolution. Development 125, 2701–2710.
Gordh, G., Headrick, D., 2011. A Dictionary of Entomology. CABI, Oxfordshire p. 2.
Halder, G., Callaerts, P., Gehring, W.J., 1995. Induction of ectopic eyes by targeted expression of the *eyeless* gene in *Drosophila*. Science 267, 1788–1792.
Hanson, I., Van Heyningen, V., 1995. *Pax6*: more than meets the eye. Trends Genet. 11, 268–272.
Hanson, I.M., 2003. PAX6 and congenital eye malformations. Pediatr. Res. 54, 791–796.
Hauck, B., Gehring, W.J., Walldorf, U., 1999. Functional analysis of an eye specific enhancer of the *eyeless* gene in *Drosophila*. Proc. Natl. Acad. Sci. USA 96, 564–569.
Hill, R.E., Favor, J., Hogan, B.L., Ton, C.C., Saunders, G.F., Hanson, I.M., Prosser, J., Jordan, T., Hastie, N.D., van Heyningen, V., 1991. Mouse *small eye* results from mutations in a paired-like homeobox-containing gene. Nature 354, 522–525.
Hogan, B.L., Horsburgh, G., Cohen, J., Hetherington, C.M., Fisher, G., Lyon, M.F., 1986. Small eyes (Sey): a homozygous lethal mutation on chromosome 2 which affects the differentiation of both lens and nasal placodes in the mouse. J. Embryol. Exp. Morphol. 97, 95–110.
Kessel, M., Gruss, P., 1990. Murine developmental control genes. Science 249, 374–379.
Klingler, M., 2004. Tribolium. Curr Biol 14, R639–640.
Kozmik, Z., 2008. The role of Pax genes in eye evolution. Brain Res. Bull. 75, 335–339.
Kronhamn, J., Frei, E., Daube, M., Jiao, R., Shi, Y., Noll, M., Rasmuson-Lestander, A., 2002. Headless flies produced by mutations in the paralogous *Pax6* genes *eyeless* and *twin of eyeless*. Development 129, 1015–1026.
Lee, H., Khan, R., O'Keefe, M., 2008. Aniridia: current pathology and management. Acta Ophthalmol. 86, 708–715.
Liu, Z., Friedrich, M., 2004. The *Tribolium* homologue of *glass* and the evolution of insect larval eyes. Dev. Biol. 269, 36–54.
Liu, Z., Yang, X., Dong, Y., Friedrich, M., 2006. Tracking down the "head blob": comparative analysis of *wingless* expression in the developing insect procephalon reveals progressive reduction of embryonic visual system patterning in higher insects. Arthropod Struct. Dev. 35, 341–356.
Lorenzen, M.D., Berghammer, A.J., Brown, S.J., Denell, R.E., Klingler, M., Beeman, R.W., 2003. piggyBac-mediated germline transformation in the beetle *Tribolium castaneum*. Insect Mol. Biol. 12, 433–440.
Lowe, C.J., Wu, M., Salic, A., Evans, L., Lander, E., Stange-Thomann, N., Gruber, C.E., Gerhart, J., Kirschner, M., 2003. Anteroposterior patterning in hemichordates and the origins of the chordate nervous system. Cell 113, 853–865.
Manuel, M., Price, D.J., 2005. Role of *Pax6* in forebrain regionalization. Brain Res. Bull. 66, 387–393.
Niederfuhr, A., Hummerich, H., Gawin, B., Boyle, S., Little, P.F., Gessler, M., 1998. A sequence-ready 3-Mb PAC contig covering 16 breakpoints of the Wilms tumor/aniridia region of human chromosome 11p13. Genomics 53, 155–163.
Ntini, E., Wimmer, E.A., 2011. Unique establishment of procephalic head segments is supported by the identification of cis-regulatory elements driving segment-specific segment polarity gene expression in *Drosophila*. Dev. Genes Evol. 221, 1–16.
Ober, K.A., Jockusch, E.L., 2006. The roles of *wingless* and *decapentaplegic* in axis and appendage development in the red flour beetle, *Tribolium castaneum*. Dev. Biol. 294, 391–405.
Osumi, N., Hirota, A., Ohuchi, H., Nakafuku, M., Iimura, T., Kuratani, S., Fujiwara, M., Noji, S., Eto, K., 1997. Pax-6 is involved in the specification of hindbrain motor neuron subtype. Development 124, 2961–2972.
Osumi, N., Shinohara, H., Numayama-Tsuruta, K., Maekawa, M., 2008. Concise review: *Pax6* transcription factor contributes to both embryonic and adult neurogenesis as a multifunctional regulator. Stem Cells 26, 1663–1672.
Passamaneck, Y.J., Furchheim, N., Hejnol, A., Martindale, M.Q., Luter, C., 2011. Ciliary photoreceptors in the cerebral eyes of a protostome larva. EvoDevo 2, 1–18.
Patel, M., Farzana, L., Robertson, L.K., Hutchinson, J., Grubbs, N., Shepherd, M.N., Mahaffey, J.W., 2007. The appendage role of insect *disco* genes and possible implications on the evolution of the maggot larval form. Dev. Biol. 309, 56–69.
Pavlopoulos, A., Berghammer, A.J., Averof, M., Klingler, M., 2004. Efficient transformation of the beetle *Tribolium castaneum* using the Minos transposable element: quantitative and qualitative analysis of genomic integration events. Genetics 167, 737–746.
Posnien, N., Bashasab, F., Bucher, G., 2009a. The insect upper lip (labrum) is a nonsegmental appendage-like structure. Evol. Dev. 11, 480–488.
Posnien, N., Bucher, G., 2010. Formation of the insect head involves lateral contribution of the intercalary segment, which depends on Tc-labial function. Dev. Biol. 338, 107–116.
Posnien, N., Koniszewski, N.D., Hein, H.J., Bucher, G., 2011. Candidate gene screen in the red flour beetle *Tribolium* reveals *six3* as ancient regulator of anterior median head and central complex development. PLoS Genet. 7, e1002416.
Posnien, N., Schinko, J., Grossmann, D., Shippy, T.D., Konopova, B., Bucher, G., 2009b. RNAi in the red flour beetle (*Tribolium*). Cold Spring Harb Protoc, pdb prot5256.
Posnien, N., Schinko, J.B., Kittelmann, S., Bucher, G., 2010. Genetics, development and composition of the insect head—a beetle's view. Arthropod Struct. Dev. 39, 399–410.
Pratt, T., Price, D.J., 2006. Dual roles of transcription factors in forebrain morphogenesis and development of axonal pathways. In: Erzurumlu, R., Guido, W., Moltan, Z. (Eds.), Development and Plasticity in Sensory Thalamus and Cortex. Springer, New York, pp. 19–41.
Quigley, I.K., Xie, X., Shankland, M., 2007. Hau-*Pax6*A expression in the central nervous system of the leech embryo. Devel. Genes Evol. 217, 459–468.
Quiring, R., Walldorf, U., Kloter, U., Gehring, W.J., 1994. Homology of the *eyeless* gene of *Drosophila* to the *Small eye* gene in mice and *Aniridia* in humans. Science 265, 785–789.
Richards, S., Gibbs, R.A., Weinstock, G.M., Brown, S.J., Denell, R., Beeman, R.W., Gibbs, R., Bucher, G., Friedrich, M., Grimmelikhuijzen, C.J., Klingler, M., Lorenzen, M., Roth, S., Schroder, R., Tautz, D., Zdobnov, E.M., Muzny, D., Attaway, T., Bell, S., Buhay, C.J., Chandrabose, M.N., Chavez, D., Clerk-Blankenburg, K.P., Cree, A., Dao, M., Davis, C., Chacko, J., Dinh, H., Dugan-Rocha, S., Fowler, G., Garner, T.T., Garnes, J., Gnirke, A., Hawes, A., Hernandez, J., Hines, S., Holder, M., Hume, J., Jhangiani, S.N., Joshi, V., Khan, Z.M., Jackson, L., Kovar, C., Kowis, A., Lee, S., Lewis, L.R., Margolis, J., Morgan, M., Nazareth, L.V., Nguyen, N., Okwuonu, G., Parker, D., Ruiz, S.J., Santibanez, J., Savard, J., Scherer, S.E., Schneider, B., Sodergren, E., Vattahil, S., Villasana, D., White, C.S., Wright, R., Park, Y., Lord, J., Oppert, B., Brown, S., Wang, L., Weinstock, G., Liu, Y., Worley, K., Elsik, C.G., Reese, J.T., Elhaik, E., Landan, G., Graur, D., Arensburger, P., Atkinson, P., Beidler, J., Demuth, J.P., Drury, D.W., Du, Y.Z., Fujiwara, H., Maselli, V., Osanai, M., Robertson, H.M., Tu, Z., Wang, J.J., Wang, S., Song, H., Zhang, L., Werner, D., Stanke, M., Morgenstern, B., Solovyev, V., Kosarev, P., Brown, G., Chen, H.C., Ermolaeva, O., Hlavina, W., Kapustin, Y., Kiryutin, B., Kitts, P., Maglott, D., Pruitt, K., Sapojnikov, V., Souvorov, A., Mackey, A.J., Waterhouse, R.M., Wyder, S., Kriventseva, E.V., Kadowaki, T., Bork, P., Aranda, M., Bao, R., Beermann, A., Berns, N., Bolognesi, R., Bonneton, F., Bopp, D., Butts, T., Chaumot, A., Denell, R.E., Ferrier, D.E., Gordon, C.M., Jindra, M., Lan, Q., Lattorff, H.M., Laudet, V., von Levetsow, C., Liu, Z., Lutz, R., Lynch, J.A., da Fonseca, R.N., Posnien, N., Reuter, R., Schinko, J.B., Schmitt, C., Schoppmeier, M., Shippy, T.D., Simonnet, F., Marques-Souza, H., Tomoyasu, Y., Trauner, J., Van der Zee, M., Vervoort, M., Wittkopp, N., Wimmer, E.A., Yang, X., Jones, A.K., Sattelle, D.B., Ebert, P.R., Nelson, D., Scott, J.G., Muthukrishnan, S., Kramer, K.J., Arakane, Y., Zhu, Q., Hogenkamp, D., Dixit, R., Jiang, H., Zou, Z., Marshall, J., Elpidina, E., Vinokurov, K., Oppert, C., Evans, J., Lu, Z., Zhao, P., Sumathipala, N., Altincicek, B., Vilcinskas, A., Williams, M., Hultmark, D., Hetru, C., Hauser, F., Cazzamali, G., Williamson, M., Li, B., Tanaka, Y., Predel, R., Neupert, S., Schachtner, J., Verleyen, P., Raible, F., Walden, K.K., Angeli, S., Foret, S., Schuetz, S., Maleszka, R., Miller, S.C., Grossmann, D., 2008. The genome of the model beetle and pest *Tribolium* castaneum. Nature 452, 949–955.
Schinko, J.B., Kreuzer, N., Offen, N., Posnien, N., Wimmer, E.A., Bucher, G., 2008. Divergent functions of *orthodenticle*, *empty spiracles* and *buttonhead* in early head patterning of the beetle *Tribolium castaneum* (Coleoptera). Dev. Biol. 317, 600–613.
Schlosser, G., 2005. Evolutionary origins of vertebrate placodes: insights from developmental studies and from comparisons with other deuterostomes. J. Exp. Zool. Part B Mol. Dev. Evol. 304, 347–399.
Shaham, O., Menuchin, Y., Farhy, C., Ashery-Padan, R., 2012. *Pax6*: a multi-level regulator of ocular development. Prog. Retinal Eye Res. 31, 351–376.
Simpson, T.I., Price, D.J., 2002. *Pax6*; a pleiotropic player in development. Bioessays 24, 1041–1051.
Snodgrass, R.E., 1935. Principles of Insect Morphology. McGraw-Hill, New York.
Stoykova, A., Fritsch, R., Walther, C., Gruss, P., 1996. Forebrain patterning defects in *Small eye* mutant mice. Development 122, 3453–3465.
Strickler, A.G., Yamamoto, Y., Jeffery, W.R., 2001. Early and late changes in *Pax6* expression accompany eye degeneration during cavefish development. Dev. Genes Evol. 211, 138–144.

Sturtevant, A., 1951. A map of the fourth chromosome of *Drosophila* melanogaster, based on crossing over in triploid females. Proc. Natl. Acad. Sci. USA 37, 405.
Suzuki, T., Saigo, K., 2000. Transcriptional regulation of *atonal* required for *Drosophila* larval eye development by concerted action of *eyes absent*, *sine oculis* and *hedgehog* signaling independent of *fused kinase* and *cubitus interruptus*. Development 127, 1531–1540.
Team, R.C., 2008. R: a language and environment for statistical computing. R Foundation for Statistical Computing, Vienna, pp. 1–1731.
Treisman, J., Harris, E., Desplan, C., 1991. The paired box encodes a second DNA-binding domain in the paired homeo domain protein. Genes Dev. 5, 594–604.
Urbach, R., Technau, G.M., Breidbach, O., 2003. Spatial and temporal pattern of neuroblasts, proliferation, and Engrailed expression during early brain development in *Tenebrio molitor* L. (Coleoptera). Arthropod Struct. Dev. 32, 125–140.
Walther, C., Gruss, P., 1991. Pax-6, a murine paired box gene, is expressed in the developing CNS. Development 113, 1435–1449.
Walther, C., Guenet, J.-L., Simon, D., Deutsch, U., Jostes, B., Goulding, M.D., Plachov, D., Balling, R., Gruss, P., 1991. Pax: a murine multigene family of paired box-containing genes. Genomics 11, 424–434.
Wheeler, S.R., Carrico, M.L., Wilson, B.A., Skeath, J.B., 2005. The *Tribolium* columnar genes reveal conservation and plasticity in neural precursor patterning along the embryonic dorsal-ventral axis. Dev. Biol. 279, 491–500.
Wright, K., 2006. Corrgram: plot a correlogram. R package version, 0.1 Ed.
Xu, P.X., Zhang, X., Heaney, S., Yoon, A., Michelson, A.M., Maas, R.L., 1999. Regulation of *Pax6* expression is conserved between mice and flies. Development 126, 383–395.
Yang, X., Weber, M., Zarinkamar, N., Posnien, N., Friedrich, F., Wigand, B., Beutel, R., Damen, W.G., Bucher, G., Klingler, M., Friedrich, M., 2009a. Probing the *Drosophila* retinal determination gene network in *Tribolium* (II): The *Pax6* genes *eyeless* and *twin of eyeless*. Dev. Biol. 333, 215–227.
Yang, X., Zarinkamar, N., Bao, R., Friedrich, M., 2009b. Probing the *Drosophila* retinal determination gene network in *Tribolium* (I): The early retinal genes *dachshund*, *eyes absent* and *sine oculis*. Dev. Biol. 333, 202–214.
Zhang, T., Ranade, S., Cai, C.Q., Clouser, C., Pignoni, F., 2006. Direct control of neurogenesis by selector factors in the fly eye: regulation of *atonal* by Ey and So. Development 133, 4881–4889.
Zhao, X., Coptis, V., Farris, S., 2008. Metamorphosis and adult development of the mushroom bodies of the red flour beetle, *Tribolium castaneum*. Dev. Neurobiol. 68, 1487–1502.
Zhou, Q., Zhang, T., Jemc, J.C., Chen, Y., Chen, R., Rebay, I., Pignoni, F., 2014. Onset of *atonal* expression in *Drosophila* retinal progenitors involves redundant and synergistic contributions of Ey/*Pax6* and So binding sites within two distant enhancers. Dev. Biol. 386, 152–164.